



Leveraging soil diversity to mitigate hydrological extremes with nature-based solutions in productive catchments

Benjamin Guillaume^{1*}, Adrien Michez^{1*}, Aurore Degré¹

¹ Uliège – Gembloux Agro-Bio Tech, TERRA Teaching and Research Centre, Passage des Déportés 2,

5 5030 Gembloux, Belgium

* These authors contributed equally to this work

Correspondence to: Benjamin Guillaume (Benjamin.guillaume@uliege.be) and Adrien Michez (adrien.michez@uliege.be)

Abstract. Nature-based solutions (NbS) are increasingly being explored as effective strategies for mitigating hydrological extremes, such as floods and agricultural droughts. Among these, soil-vegetation-based approaches may play a key role in improving soil health, enhancing ecosystem services, and restoring the natural hydrological cycle in productive agricultural and forestry catchments, making these landscapes more resilient to climate change. However, the influence of local factors, such as soil characteristics, on the effectiveness of these interventions is often overlooked. This study investigates the role of spatial variability of soil properties in shaping the effectiveness of NbS for mitigating both floods and agricultural droughts. To this end, two distributed, physically based hydrological models, one for an agricultural catchment and one for a forest dominated catchment, were developed, integrating two landscape planning scenarios involving a series of NbS to be represented. Key spatially based indicators to assess the effectiveness of NbS were developed based on long term simulation results. A major output from this study is that the effectiveness of NbS in improving flood and drought resilience is dependent on the soil's natural drainage characteristics, with well-drained soils demonstrating the greatest potential. In well-drained soils, hedgerows significantly enhanced infiltration by improving soil hydraulic properties and creating additional air space in the soil's porosity through higher rates of evapotranspiration. In contrast, improving hydraulic properties in waterlogged soils had minimal impact on infiltration due to existing saturation, with anoxic conditions potentially limiting transpiration. Additionally, the study highlights that well-drained soils offer co-benefits for resilience to agricultural droughts, as they are more likely to experience water deficits that NbS can mitigate. In contrast, such benefits are generally absent in waterlogged soils, which rarely face water scarcity. Future approaches to evaluate the potential effectiveness of NbS should recognize the spatial variability in their performance. This variability should inform the type and location of NbS to increase their overall effectiveness.

1 Introduction

Central Europe faced consecutive abnormally dry and hot summers in 2018, 2019, and 2020 (van der Wiel et al., 2023). The drought event of 2018–2019 was considered unprecedented in the last 250 years (Hari et al., 2020), adversely impacting agricultural productivity (Toreti et al., 2019). Droughts are classified as meteorological, agricultural, hydrological, or



socioeconomic. Meteorological drought refers to a deficiency in rainfall, while agricultural drought, driven by soil moisture deficits, occurs when soil water availability does not meet plant requirements. It is therefore influenced by vegetation characteristics, as species differ in their sensitivity to the same soil moisture deficit. Extended rainfall shortages may result in hydrological drought, affecting streamflow and aquifers, eventually causing socioeconomic drought when water supply fails to meet demand (Mishra and Singh, 2010).

Conversely, the same region, comprising western Germany, eastern Belgium, Luxembourg, and the Netherlands, experienced a very wet 2021 summer and an extreme precipitation event between July 13 and 16, with unprecedented accumulations. Combined with already nearly saturated soil conditions, this extreme rainfall event led to major floods, making it one of the most severe natural catastrophes in Europe of the past half-century (Journée et al., 2023).

Due to the anthropogenic global warming and the demographic expansion, the likelihood of occurrence and impact of droughts and floods is expected to be exacerbated (Aalbers et al., 2023; Dottori et al., 2023; Hari et al., 2020), consequently increasing the associated damage costs (Naumann et al., 2021), currently estimated at €9 billion for droughts (Cammalleri et al., 2020) and €7.6 billion for floods (Dottori et al., 2023) annually in the European Union.

In order to mitigate and potentially reverse these adverse effects, investments in a transformative adaptation of human systems are required (Pörtner et al., 2022). Given the uncertainty of future climate conditions, these investments could prioritize soft strategies, "no regret" approaches which yield benefits irrespective of climate change, as well as reversible and flexible options, providing significant social, economic and environmental benefits (Hallegatte, 2009). In line with this philosophy, the recently introduced umbrella concept of nature-based solutions (NbS) is becoming increasingly popular among funders, researchers, policy makers and practitioners (Nesshöver et al., 2017). NbS could be referred to as solutions rooted in natural processes and ecosystems, designed to address a spectrum of societal and environmental challenges, including hydro-meteorological risks reduction (Ruangpan et al., 2020).

While NbS literature is abundant on runoff and flood risk reduction in urban areas (Ruangpan et al., 2020), there has been limited exploration of NbS as drought mitigation strategies (Yimer et al., 2024). Furthermore, potential combined effects, such as synergies and trade-offs of NbS on floods and droughts, remain largely unexplored (Fennell et al., 2023b; Penning et al., 2023). NbS are frequently considered effective in addressing hydrological droughts (Fennell et al., 2023a), and less so for agricultural droughts. However, NbS are increasingly recognized as a useful concept extending beyond the urban/riverine context, such as in agricultural or forest settings (Hanson et al., 2020) to improve drought resilience of these ecosystems while contributing to reduce flood risks. In these contexts, NbS may include soil-vegetation solutions aimed at enhancing soil health, functions and ecosystem services with agronomic and/or forest management practices and/or land restoration. Other NbS also referring to as "landscape solutions" aim at hydrologically disconnecting watersheds (Keesstra et al., 2018). However, in these alternative land use contexts such as agriculture or forestry, the effectiveness of NbS might highly depend on local characteristics such as the infiltration capacity of the soil (Fennell et al., 2023a; Penning et al., 2023). Indeed, soil hydraulic properties and their spatial distribution play a crucial role in controlling small-scale (soil profile scale)



hydrological processes within a watershed (Vereecken et al., 2022) and consequently, the small-scale effectiveness of NbS
65 influencing hydrological processes within a watershed.

This fine-scale spatial variability raises important questions about the appropriate methods and scales to assess and monitor
the effectiveness of these interventions before and after implementation. One popular approach for assessing the potential
effectiveness of NbS before implementation for floods and droughts involves modelling hydrological, hydraulic, and water
balance processes. This approach often involves comparing the modelled outcomes of a baseline scenario of the current
70 conditions, to a target scenario (Possantti and Marques, 2022). In the urban context, the hydrological effectiveness of NbS is
often assessed downstream through simulated discharge series using empirical or conceptual (sometimes lumped) rainfall
runoff models (Possantti et Marques, 2022; Kumar et al., 2021). However, this type of evaluation does not differentiate the
effectiveness of individual upstream interventions, ignoring the significance of the spatial arrangement of NbS within the
watershed. This oversight presupposes that it has a minimal impact on their effectiveness downstream, as identified in the
75 case of green roofs (Qiu et al., 2021).

This consideration opens the door for spatially distributed, physically based hydrological modelling approaches, able to rank
most effective NbS-locations combinations in a given context (Brauman et al., 2022). Indeed, these types of models enable
the virtual implementation of a set of NbS at the catchment scale with a specific spatial arrangement. Water fluxes,
calculated on a variable-resolution grid, are derived from physically meaningful equations that rely on physically meaningful
80 local parameters that can be measured (topography, geology, soil hydraulic properties, surface roughness, vegetation). These
factors influence small-scale (grid cell scale) hydrological processes, such as infiltration. Through the spatial and temporal
adjustment of these parameters, scenarios of NbS can be represented. Thus, the physical response (and effectiveness) of an
intervention implemented at a specific location that might affect the global catchment's behaviour can be modelled.

This article introduces a reproducible methodology for developing a physically based surface hydrological model designed
85 to evaluate the impact of NbS scenarios at the catchment scale. Serving as a foundational step, this modelling framework
facilitates a series of innovative post-processing analyses to assess NbS hydrological effectiveness. The paper addresses
three key objectives: i) Moving beyond a simple analysis of outflow discharges by emphasizing the influence of spatial
variability in soil characteristics on the effectiveness of hydrological NbS measures inside the watershed; ii) Evaluating the
impact of NbS on different hydrological extremes, specifically floods and agricultural droughts; iii) Investigating synergies
90 and trade-offs between floods and agricultural droughts mitigation through NbS implementation.

2 Materials and Methods

2.1 Study area

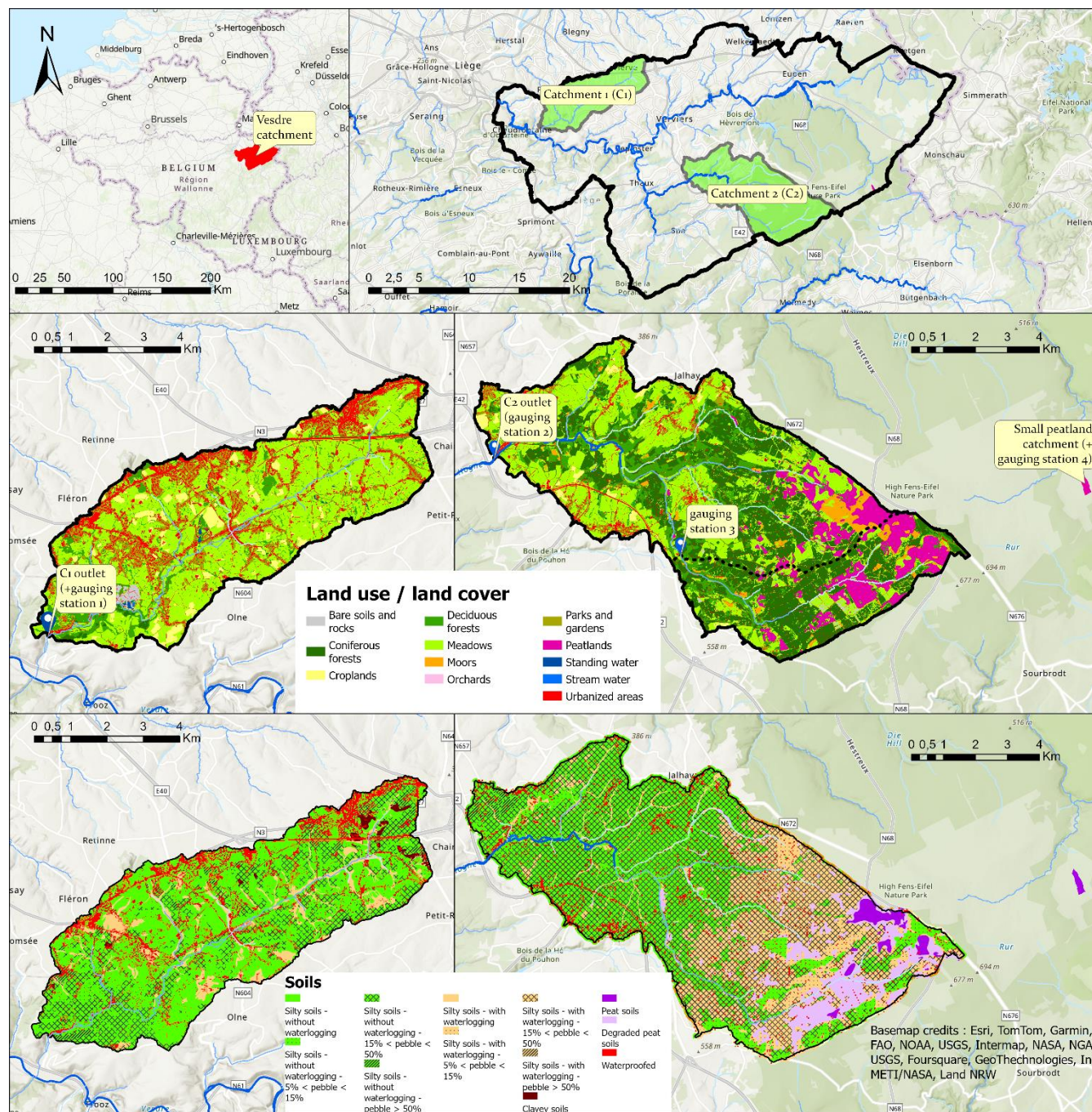


Figure 1: Study area with maps of land use/ land cover and soils.



95

To illustrate the proposed methodology, two applications are presented on sub-catchments with contrasting land uses belonging to the Vesdre catchment in Belgium. The first catchment (C1) is primarily agricultural (69 %) and peri-urban (17 %), covering 39.9 km² with altitudes ranging from 125 m to 325 m. The climate is temperate oceanic with annual precipitation rate over the catchment of 952 ± 96 mm (mean and standard deviation calculated between 2004 and 2021).

100 Soils are mostly silty, with depths ranging from 0 m to 6 m. Rock fragments are present only in the sloping soils. Natural soil drainage is moderate on the plateaus, favourable on the slopes, and poor in the valley bottoms (Table 2). The second catchment (C2) is dominated by forests (45 %), meadows (35 %) and peatlands (10 %). It spans 71 km² with elevations ranging from 350 m to 687 m. The terrain varies from relatively flat upstream on the High Fens Plateau (dominated by peatlands, wet moorlands and drained plantations of coniferous trees) to deep valleys downstream (dominated by coniferous
105 plantations, deciduous forests and meadows). The annual precipitation rate over the catchment is 1158 ± 123 mm (mean and standard deviation calculated between 2004 and 2021). Apart from peatlands, the soils are composed mainly of silts with a variable stone content. On the upstream plateaus, soils are deeper due to lower erosion rates and are more prone to waterlogging, unlike downstream well-drained soils, which typically contain a higher stone content. Since the latter half of the 19th century, extensive surface drainage efforts have been undertaken on the upstream plateau to facilitate the
110 establishment of conifer plantations (mainly *Picea abies*). This has resulted in the degradation of the region's open wetlands and peat soils.

2.2 Modelling Framework

2.2.1 Hydrological model

115 The model selection was based on its capability to represent long time series of multiple hydrological processes (channel flow, overland flow, unsaturated- and saturated-flow, evapotranspiration, etc) at the catchment scale using a fully distributed 3D lattice. Therefore, the coupled hydrologic/hydraulic MIKE SHE/MIKE 1D model was chosen. MIKE SHE/MIKE 1D solves partial differential physically based equations describing mass and energy transfers. The actual evapotranspiration is derived from the reference evapotranspiration using the Kristensen and Jensen method. 2D overland flow is calculated using
120 the diffusive wave approximation of the Saint-Venant equations. 1D Channel flow is derived from the fully dynamic higher order approximation of the Saint-Venant equations. 1D Unsaturated flow is derived from the Richards equation. Saturated flow is described by the 3D Darcy's equation numerically solved using the finite difference method (DHI, 2024).

Hydrometeorological data: The climate data comprised a 5 x 5 km grid detailing hourly precipitation intensities and daily
125 reference evapotranspiration. Reference evapotranspiration was estimated using the Penman-Monteith equation (Allan et al., 1998) applied to data collected by the observation network of the Belgian Royal Meteorological Institute (RMI), including



temperature, humidity, wind speed, and solar radiation (« Gridded observational data »). Precipitations were determined by combining RMI's gridded daily data with hourly point measurements from the Wallonia Public Service's rain gauge network (<https://hydrometrie.wallonie.be>), enabling the hourly distribution of RMI's daily rainfall data.

130 Hourly stream discharge data were obtained from 11 May 2011 at the outlet of C1 (gauging station 1), from 30 November 2015 at the outlet of C2 (gauging station 2) and from 1 January 2000 in an upstream branch of C2 with (gauging station 3) a drained area of 19.6 km² (<https://hydrometrie.wallonie.be>).

135 Topographic data: The topographic data were a hydrologically corrected Digital Elevation Model (DEM) at a 2m resolution (LIDAXES (version 2) - MNT, 2023). Resampling onto the model grid involves selecting the minimum elevation value to maintain the hydrological correction applied.

140 Land cover – land use data: Land use/land cover (LULC) information was used to define spatially variable surface roughness and vegetations. The LULC map was a 5 m resolution layer of the land cover of 2018 (WALOUS 2018 - Série, 2024; Bassine et al., 2020) mapping several LULC classes. Resampling onto the model grid was performed by selecting the predominant LULC within each grid cell. Each LULC class was assigned an M value of Manning.

145 The surfaces were also categorized into seven vegetation classes based on the LULC map. Each vegetation class was assigned annual dynamics (temporally varying) of leaf area index (LAI), crop coefficient factor (Kc), and root depth (Rd) (Figure - A1) These parameters are used by the model to refine the reference evapotranspiration (Penman-Monteith) into the actual evapotranspiration following the approach of Kristensen and Jensen (DHI, 2024). In addition, detention storage, which is a parameter aimed at accounting for ponding in depressions at sub-cell scale, was fixed to 4 mm in both catchments.

Table 1: Equivalences between land use / land cover classes and vegetation classes.

Vegetation class	Land use / land cover class	Maximum rooting depth (cm)
No vegetation	Railway network, road network, above ground artificial construction, artificial ground covering, and bare soil	0
Wetland	Bog, lake, pond, pool, basin, wet heathland, river surface, and other unclassified water surface	10
Open production surfaces	Herbaceous cover in rotation within the year, herbaceous cover all year round, forage crop, hay meadow, wet meadow, permanent meadow, intensive permanent meadow, orchard, nuts and other herbaceous cover all year round	50
Coniferous Forests	Spruce forest, Douglas fir forest, pine forest, conifers,	60



	conifers < 3m, conifers > 3m, Christmas tree, and other coniferous stand or unknown resinous essence > 3m	
Deciduous Forests	Deciduous trees, deciduous trees < 3m, deciduous trees > 3m, birch forest, oak forest, beech forest, larch forest, poplar forest, other deciduous stand or unknown deciduous essence > 3m	120
Open conservation zones	Dry heathland and dry grassland	50
Croplands	Corn, cereal and similar, beetroot, chicory, potato, vegetable, oilseed and other crops or other agricultural uses	40

Soil and subsoil data: The 1D Richards equation was used to model vertical water fluxes in the unsaturated zone, which
 150 required the determination of the soil hydrodynamic properties (soil water retention and soil hydraulic conductivity curves) using the Van Genuchten and Mualem functions (Van Genuchten, 1980) at each location within the unsaturated zone. Saturated flow was modelled with the 3D Darcy's equation requiring vertical and horizontal saturated conductivities to be specified at each location within the saturated zone.

The soil and subsoil were represented as a series of layers with homogeneous hydrodynamic properties within each layer, but
 155 varying between layers in terms of thickness and lateral arrangement. Except for peat and degraded peat soils, the upper soil profile was discretized into two layers: topsoil, ranging from 0 m to 0.4 m, and subsoil, extending from 0.4 m to a maximum of 2 m deep. These two layers could be truncated by the base at depths of 0.2 m, 0.3 m, or 0.6 m, considering the soil depth information from the Belgian soil map (« Carte Numérique des Sols de Wallonie »).

The upper soil profile was delineated into homogeneous units based on the Belgian soil map (Figure 1) (« Carte Numérique
 160 des Sols de Wallonie »). This map is derived from approximately 6 000 000 samplings conducted with a soil auger (max 1.25 m depth) between 1947 and 1991 of the Belgian cadastral plans, according to a square grid of 75 m per side (1 to 2.5 observations per hectare). This map delineates 6000 soil units defined by characteristics such as texture, natural drainage, diagnostic horizon, and stone content (Legrain et al., 2011). For each homogeneous unit, excepted for peat, degraded peat and impermeable soils, retention and hydraulic conductivity curves (Van Genuchten and Mualem models, with $m = 1-1/n$ and $L = 0.5$) for both soil layers were derived from the European hydraulic pedotransfer function (euptfv2) number 1 using
 165 depth and the averaged soil texture (« Textures et fractions granulométriques de référence des sols de Wallonie - Série ») as predictors (Szabó et al., 2021). The predicted saturated water content, θ_s , was subsequently corrected to account for the loss of porosity due to stone content, s , as represented in the Belgian soil map.

$$\theta_{s-pebble} = \theta_s(1 - s), \quad (1)$$



170 For the peat soil units, retention curves were obtained by measurements of water content on peat samples of local bogs using
pressure plates at pF values of 1.00, 1.60, 1.85, 2.00, 2.30, 2.78, 2.95, 3.62, 4.14. Van Genuchten functions were then
adjusted to measured retention curves. The saturated hydraulic conductivity of peat is spatially highly variable and
challenging to measure in laboratory. Saturated hydraulic conductivity was initially determined based on values found in the
literature (Wastiaux, 2008). As suggested by Szabó et al. (2024), it was subsequently refined through calibration using
175 discharge measurements conducted between 2012 and 2015 at the outlet (gauging station 4) of a small peatland catchment of
14 hectares, located 5 km away from C2. The thickness of the degraded peat soil unit was assumed to be 0.4 m, while the
peat soil unit was assumed to be 2 m thick. Beneath peat or degraded peat, a low-permeability layer of 0.6 m thickness with
60 % clay, 35 % silt, and 5 % sand was assumed, and its hydrodynamic parameters are retrieved using euptfv2.

Below the upper soil profile, multiple geological units extending to a depth of 18 m were delineated based on a 1x1 km grid.
180 Each geological unit consisted of multiple layers, exhibiting variations in thickness and vertical hydraulic conductivity.
These values were defined through a bibliographic study of the hydrogeological context of the Vesdre catchment (Sohier,
2011). Due to their imprecise nature and large spatial variability, vertical hydraulic conductivities were initially defined as
ranges of plausible values and were subsequently refined during the model calibration process. Horizontal hydraulic
conductivities were assumed to be 10 times greater than vertical hydraulic conductivities (DHI, 2024).

185
Models' specification, calibration and validation: For both catchments, a model of the present situation (further referred to as
BASELINE) was calibrated and validated. The total simulation period was comprised between 1 January 2002 and 31
December 2021. At the start of the simulation process, the soil water content was set to field capacity. The first two years of
simulation were considered a warming period and were not considered in the data analysis. Outputs were stored on an hourly
190 basis. To ensure a fine representation of the catchments while maintaining reasonable computational times, the grid
resolution of the C1 model was 20 m, whereas it was 40 m for the C2 model. Calibration was conducted in the period
between 1 October 2017 and 1 October 2021, while validation encompassed the remaining available data.

The calibration was performed manually and limited to very few parameters, for which the available data were considered
uncertain and had the most impact (the most sensitive parameters) on the modelled hydrographs. These parameters included
195 the Manning's M roughness coefficients for overland and channel flows (which are mostly sensitive regarding the
temporality of hydrographs and peak flows), as well as the saturated hydraulic conductivity of the geological layers (which
are sensitive regarding baseflow, peak discharge values, and groundwater head) (XEVI et al., 1997). Calibration of the
Manning's M roughness and the saturated hydraulic conductivities of peat were performed using discharge measurements
conducted between 2012 and 2015 at the outlet of the small peatland catchment of 14 hectares (gauging station 4).
200 Calibration and validation were performed in relation to historical discharge measurements taken at the river gauging
stations. The ability of the model to reproduce observed discharges was assessed against the Moriasi et al. (2007) model
evaluation guidelines. This included the computation of the Nash-Sutcliffe Efficiency (NSE), the ratio of the root mean
square error to the standard deviation of measured data (RSR), and the percent bias (PBIAS).



$$NSE = 1 - \frac{\sum_i(QObs_i - QMod_i)^2}{\sum_i(QObs_i - \frac{\sum_t QObs_i}{n})^2}, \quad (2)$$

205 NSE varies from $-\infty$ to 1. The closer to 1 the better the simulation performance. $QObs$ and $QMod$ are the observed and simulated discharges, respectively. i is the time step.

$$RSR = \frac{RMSE}{STDEV_{obs}} = \frac{\sqrt{\sum_i(QObs_i - QMod_i)^2}}{\sqrt{\sum_i(QObs_i - \frac{\sum_t QObs_i}{n})^2}}, \quad (3)$$

RSR varies from 0 to $+\infty$. The closer to 0 the better the simulation performance.

$$PBIAS = \frac{\sum_i(QObs_i - QMod_i) * 100}{\sum_t QObs_i}, \quad (4)$$

210 PBIAS varies from $-\infty$ to $+\infty$. The closer to 0 the better the simulation performance. Positive values indicated model underestimation bias, and negative values indicated model overestimation bias.

In the absence of piezometric data at the study sites, a visual assessment of the simulated vertical dynamics of the saturated zone was conducted on soils of each drainage class of the Belgian soil map (Table 2). This ensured that the modelled saturated zone dynamics match those described by the soil map. Drainage class is a concept used in different soil classifications to describe the frequency and duration of soil wetness under natural conditions (Ditzler, 1999). In the Belgian soil classification, drainage classes are determined by the depth at which mottling and reduction processes occur in the soil profile, often corresponding to the levels of saturated zone fluctuations (Table 2). This method facilitates semi-quantitative spatial validation across the entire catchments' areas.

215

Table 2: Definition of the drainage class in the Belgian soil classification for loam and clay soils.

		Depth (cm) at which mottling and reduction features start	
Natural drainage class for clay and silt soils		Mottling	Reduction
Without waterlogging	Favourable	>125	-
	Moderate	80-125	-
	Imperfect	50-80	-
Temporarily waterlogging	Quite poor	30-50	-
	Poor	0-30	-
Permanent waterlogging	Quite poor	30-50	>80
	Poor	0-30	40-80
	Very poor	-	<40

220



2.2.2 Landscape planning scenarios

The impact of NBS on catchment hydrology was evaluated through the comparison of responses between BASELINE and POST configurations, under consistent meteorological forcing. The POST landscape configuration was a scenario where soil-vegetation NBS were implemented at the scale of the entire watershed. These measures were implemented in line with the predominant land use (agricultural or forests and natural areas).

The following NbS measures were implemented in the agricultural catchment (C1) (Figure 2– a):

- Hedgerows: a dense network of hedgerows was systematically implemented around all agricultural parcels, representing around 700 km of barriers within the entire watershed ($\approx 175 \text{ m. hectare}^{-1}$) (Table 3-a).
- Agricultural practices: water and soil conservation practices were modelled on cultivated land, including soil pitting for maize crops (Table 3-c) to form small depressions between rows (0.73 km^2 or 1.8 %) (Clement et al., 2023) and the adoption of reduced tillage practices (Table 3-b) for the other crops (0.30 km^2 or 0.8 %).

In the forest catchment (C2), the following NbS measures were implemented (Figure 2- b):

- Restoration of peatlands: this involved restoring peatlands and open wetlands on degraded peaty soils, currently occupied by conifer plantations and moors (4.6 km^2 or 6.5 %). The scenario simulated the plugging of the existing surface drainage network with 275 plugs distributed along concentrated flow paths (drainage area from 2 to 5 hectares) and the creation of 32 ponds of 640 m^3 each (Table 3-f).
- Forest diversification: this scenario was complemented by forest diversification, involving the conversion of monospecific conifer plantations into irregular mixed stands on temporarily waterlogged soils (5.4 km^2 or 7.6 %) (Table 3-e).

Practices aimed at limiting soil compaction: for all forest areas, potential effect of forest practices aimed at limiting soil compaction, notably through compartmentalization with designated skid trails were incorporated into this scenario (16.8 km^2 or 23.7 %) (Table 3-d).

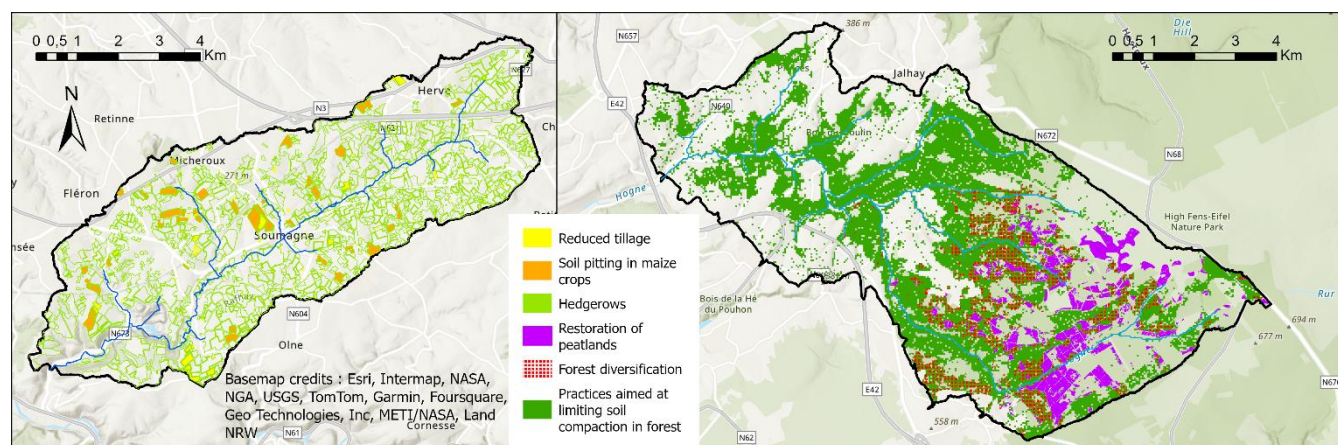


Figure 2: Modelled NbS in POST configurations of C1 and C2.

Table 3: Summary of hypotheses for parameter modifications in models to represent NbS scenarios.

Modelled NBS	Modified parameter	How modified
--------------	--------------------	--------------



a - Hedgerows	Vegetation class	from BASELINE to deciduous forest
	Manning M	from BASELINE to 2
	Saturated hydraulic conductivity of the first 40 cm of soil	100 %
	Saturated water content of the first 40 cm of soil	+ 20 %
b - Reduced tillage practices	Alpha shape parameter of the Van Genuchten's & Mualem's functions of the first 40 cm of soil	- 20 %
c - Soil pitting for maize crops	Detention storage	+ 20 mm
d - Practices aimed at limiting soil compaction in forest	Saturated hydraulic conductivity of the first 40 cm of soil	+ 50 %
	Saturated water content of the first 40 cm of soil	+ 10 %
e - forest diversification	Vegetation class	from BASELINE to deciduous forests
	Manning M	from BASELINE to 5
f - Restoration of peatlands on degraded peat soils	Vegetation class	from BASELINE to wetland
	Manning M	from BASELINE to 5
f - Plugs in the drainage network	Topography	+ 0.45 m
f - Ponds	Topography	- 0.45 m

2.2.3 Integrated hydrological analysis of model outputs

A complete processing chain of results focusing on the quantification of hydrologic impact of NbS measures and scenarios was conducted (Table 4). Hydrologic indicators were developed to capture the impact of various measures within the watershed, emphasizing the spatial variability of their effectiveness. These indicators are designed to assess how NbS could influence hydrological extremes, particularly focusing on flooding events and agricultural droughts.

Table 4: Summary of hydrological indicators aimed at assessing the effectiveness of NbS to mitigate floods and drought.

Indicator	Focus	Spatial scale of application	Temporal scale of application	Overview	Variables of interest
Outlet hydrograph	Flood	Watershed (outlet)	Every rainfall event	Modification of peak discharges and total volumes discharged	River flow rate
Infiltration	Flood	Spatially distributed (grid cell)	Every rainfall event generating > 5 mm runoff	Modifications of spatially distributed infiltration	Infiltration, seepage flow
Agricultural drought	Water stress (all types of vegetation)	Spatially distributed (grid cell)	Days to months	Modifications of consecutive days of vegetation stress considering a stress threshold and a return period	Soil water potential, root depth



Outlet hydrograph indicators: Outlet hydrograph was an integrative metric permitting to evaluate the overall effect of a given scenario without discriminating against the impact of the various measures that comprise the scenario. To this end, two flood indicators were developed for a set of rainfall events generating a detectable signal on the hydrograph. A focus was also made on the rainfall event between July 13 and July 18 of 2021:

- Peak discharges: The evolution of peak discharges between the BASELINE and the POST scenarios.

$$Peak\ discharge = 100 * \frac{Peak\ discharge_{POST} - Peak\ discharge_{BASELINE}}{Peak\ discharge_{BASELINE}}, \quad (5)$$

- Total volume discharged: The evolution of the total amount of water discharged at the outlet between the BASELINE and the POST scenarios.

$$Total\ volume = 100 * \frac{Total\ volume_{POST} - Total\ volume_{BASELINE}}{Total\ volume_{BASELINE}}, \quad (6)$$

Spatialized indicators: These indicators aimed to assess the local hydrological impact of specific NbS measures where they were located within the watershed. This allowed for discrimination of measures based on their relative impact within the same scenario. These indicators presupposed that the hydrological effects observed at a given location are exclusively attributed to the measure implemented at that site, irrespective of the presence of other measures elsewhere within the watershed.

- Infiltration: As a spatialized indicator to assess the effectiveness of NbS to mitigate flood, the cumulative infiltration, I_{cum} , between July 13 and July 18 of 2021 was displayed for each model grid cell.

$$I_{cum} = \sum_i (Infiltration_i - Seepage_i), \quad (7)$$

$Infiltration$ was the amount of water (in mm) flowing into the soil. $Seepage$ was the amount of water (in mm) outflowing from the soil. i was the time step.

- Agricultural drought: An indicator for vegetation water stress was developed, utilizing a frequency analysis. Consecutive days where plants at specific locations underwent water stress beyond a designated threshold against a return period were mapped. Thresholds were determined based on the soil water potential within the root zone. An extreme stress threshold was defined when the water potential in the root zone drops below -150 m (\approx -1.5 MPa), closely approaching the permanent wilting point which is classically recognized by soil scientists as the soil water potential beyond which most plants cannot survive (Wiecheteck et al., 2020). Additionally, a moderate stress threshold for vegetation is established at a water potential of -30 m (\approx -0.3MPa), corresponding in our study sites to approximately 30% of the relative extractable water content in soil (Gourlez de la Motte et al., 2020; Granier et al., 2007). The methodology to construct this indicator is briefly described as follows: For each cell of the model and for each year (2004-2021), the maximum consecutive duration during which the water potential in the soil profile



explored by the roots (rhizosphere) was below the stress threshold was extracted. Then, for each cell, a Gumbel distribution was used to establish the relationship between the duration (y) and the probability of occurrence (return period: TM) of the stress.

285

$$y = -c \left(\ln \ln \frac{TM}{TM-1} \right) - a, \tag{8}$$

c and a are adjustment parameters. TM corresponds to the return period and is calculated according to:

$$TM = \frac{n+1}{m}, \tag{9}$$

290

n is the rank in the descending order and m is the total number of years of observations. Once the parameters, a and c are fitted for a given stress threshold, y can be retrieved using eq. (8) (Maidment, 1992).

3 Results and Discussion

3.1 Calibration and validation of the baseline model

295

The simulated discharges evaluated at each gauging station, against Moriasi criteria, showed satisfactory to good performance (Table 5). Among the three indicators, the NSE values were the least satisfactory according to Moriasi's criteria. This could be explained by the fact that NSE is very sensitive to peak flows while measured flow rates during these events are more uncertain (well above the maximum gauged discharge on the rating curve). RSR and PBIAS were considered satisfactory/good ($0.50 < RSR < 0.60$ for good, $0.60 < RSR < 0.70$ for satisfactory) and very good ($PBIAS < \pm 10$).

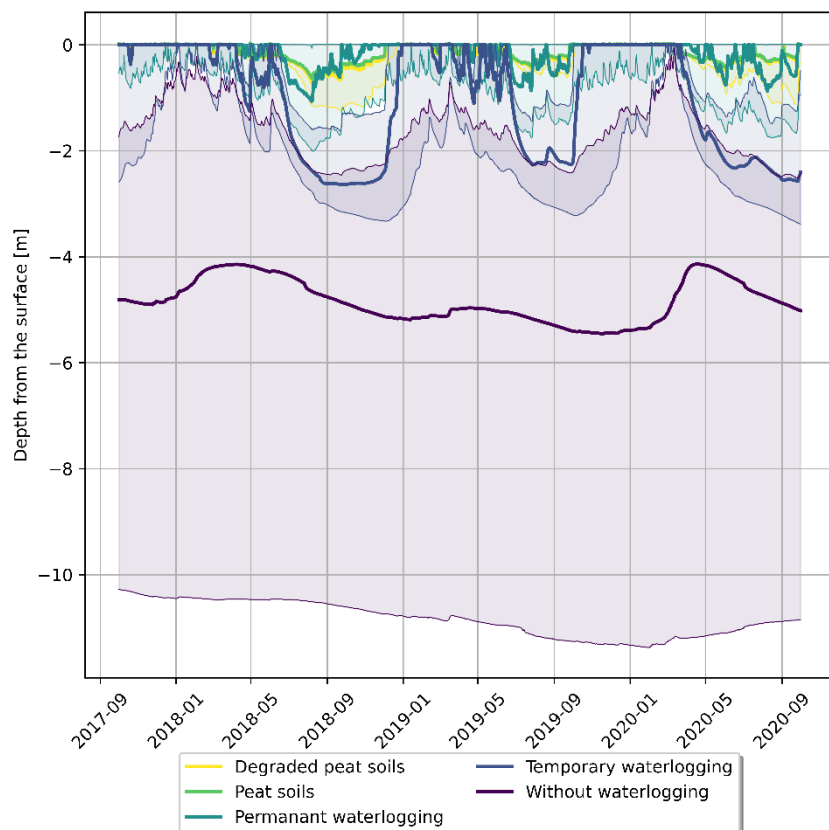
Table 5: Summary of model performance at gauging stations

	Calibration			Validation			
	NSE	RSR	PBIAS	NSE	RSR	PBIAS	Model performance
Gauging station 1	0.72	0.53	-7.2	0.64	0.60	-9.3	Satisfactory
Gauging station 2	0.69	0.55	8.0	0.65	0.59	1.5	Good
Gauging station 3	0.68	0.56	14.7	0.62	0.61	8.6	Satisfactory
Gauging station 4	0.74	0.51	8.6				

300

The modelled dynamics of the saturated zone depth agreed well with the expected dynamics for each drainage class on the Belgian soil map (Figure 3). The range of variation, as well as the frequencies of the modelled saturated zone depths, were slightly higher in the degraded peat soils compared with the intact peat (Wastiaux, 2008). Soils designated as "without waterlogging" on the soil map were seldom, if ever, subject to waterlogging. In most grid cells, the modelled saturated zone remained well below the surface, with few exceptions in late winter. As expected in temporarily waterlogged soils, the modelled saturated zone often reached the surface during the winter months and receded during the summer.

305



310 **Figure 3: Modelled saturated zone depth (watersheds C1 and C2) based on drainage classes from the Belgian soil map. The thick line represents the median values calculated from each model cells for each drainage class. The thin lines indicate the 25th and 75th percentiles.**

3.2 Effectiveness of NbS scenarios against floods at the outlets

The modelled specific peak discharges (Figure 4) indicate that, for an equal surface area, C2 generates more runoff than C1, despite C2 being predominantly forested, a land cover generally associated with lower runoff generation compared to pasture (Bathurst et al., 2020) or urbanized areas. This result may seem counterintuitive; however, C1 and C2 differ in terms of topography, morphometry, climate, geology, and soil characteristics (Figure 1), all of which can influence runoff production and transfer within a catchment.

The extreme rainfall event between 13 July and 18 July of 2021 was one of the events generating the highest peak discharge (represented by the squares in the upper part of Figure 4 in the modelled time series). The modelled hydrographs of this event in both catchments are presented in the lower part of Figure 4.

320 Landscape planning scenarios showed contrasting effectiveness in terms of reducing peak discharges between the two catchments. In C1 (mostly agricultural), peak discharges were reduced by approximately 30 %, while in C2 (forest-dominated) it was approximately 10 %. Moreover, for both catchments, the effectiveness in reducing peak discharges was

not influenced by the magnitude of the events, as indicated by the linear trend observed in the scatter plot between BASELINE and POST peak discharges. The response remained relatively consistent for both low- and high-discharge events.

325

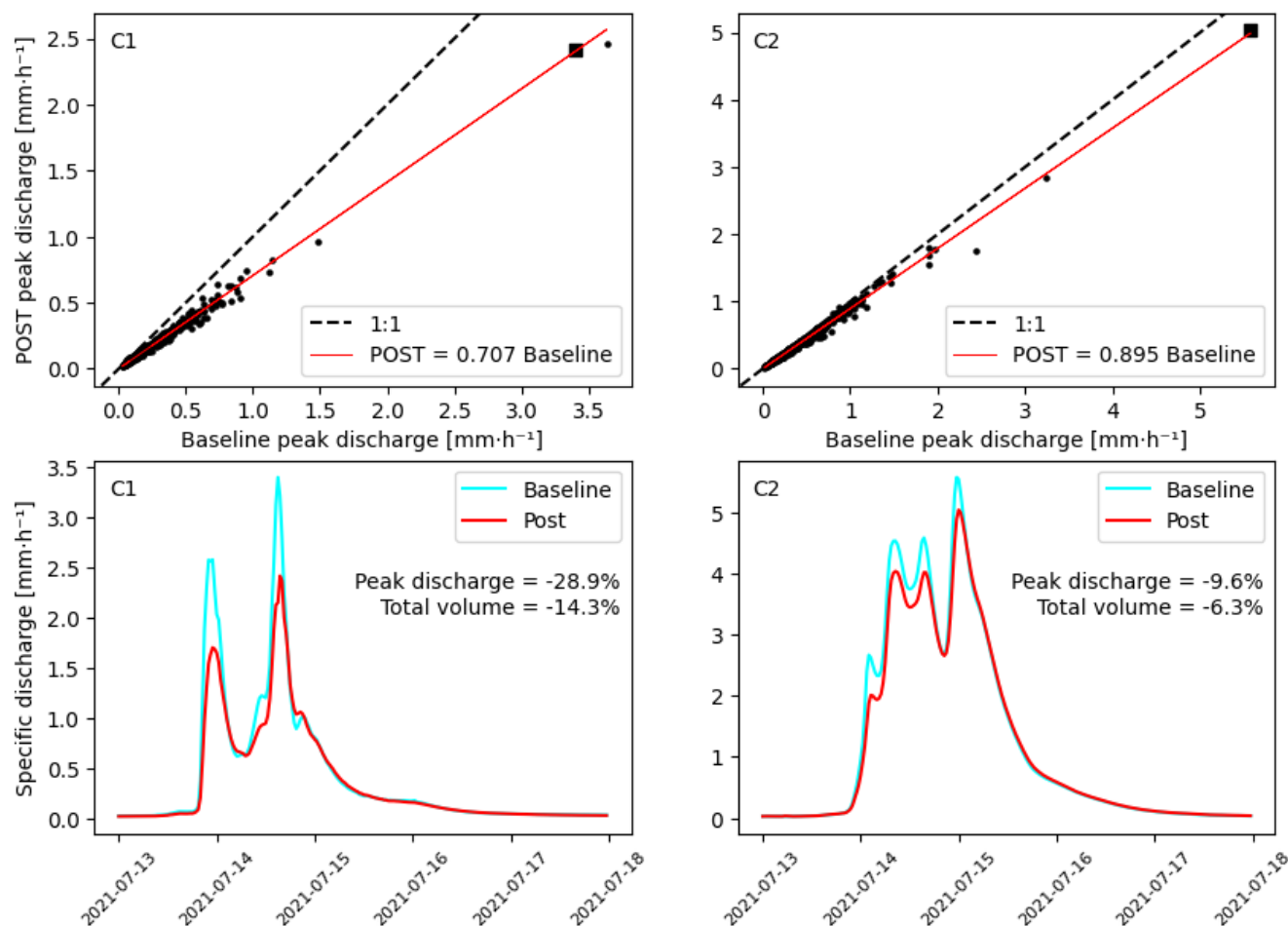


Figure 4: Modelled specific peak discharges at the outlets of C1 and C2 before and after the implementation of landscape planning scenarios. The top section shows scatter plots illustrating the evolution of peak discharges for a large number of runoff events between 2004 and 2021. The regression slope coefficients indicate the average reduction in peak flow. The squared dot highlights the peak discharge of the event occurring between 13 July and 18 July 2021. The bottom section presents hydrographs of this specific event, comparing conditions before and after the implementation of the landscape planning scenario.

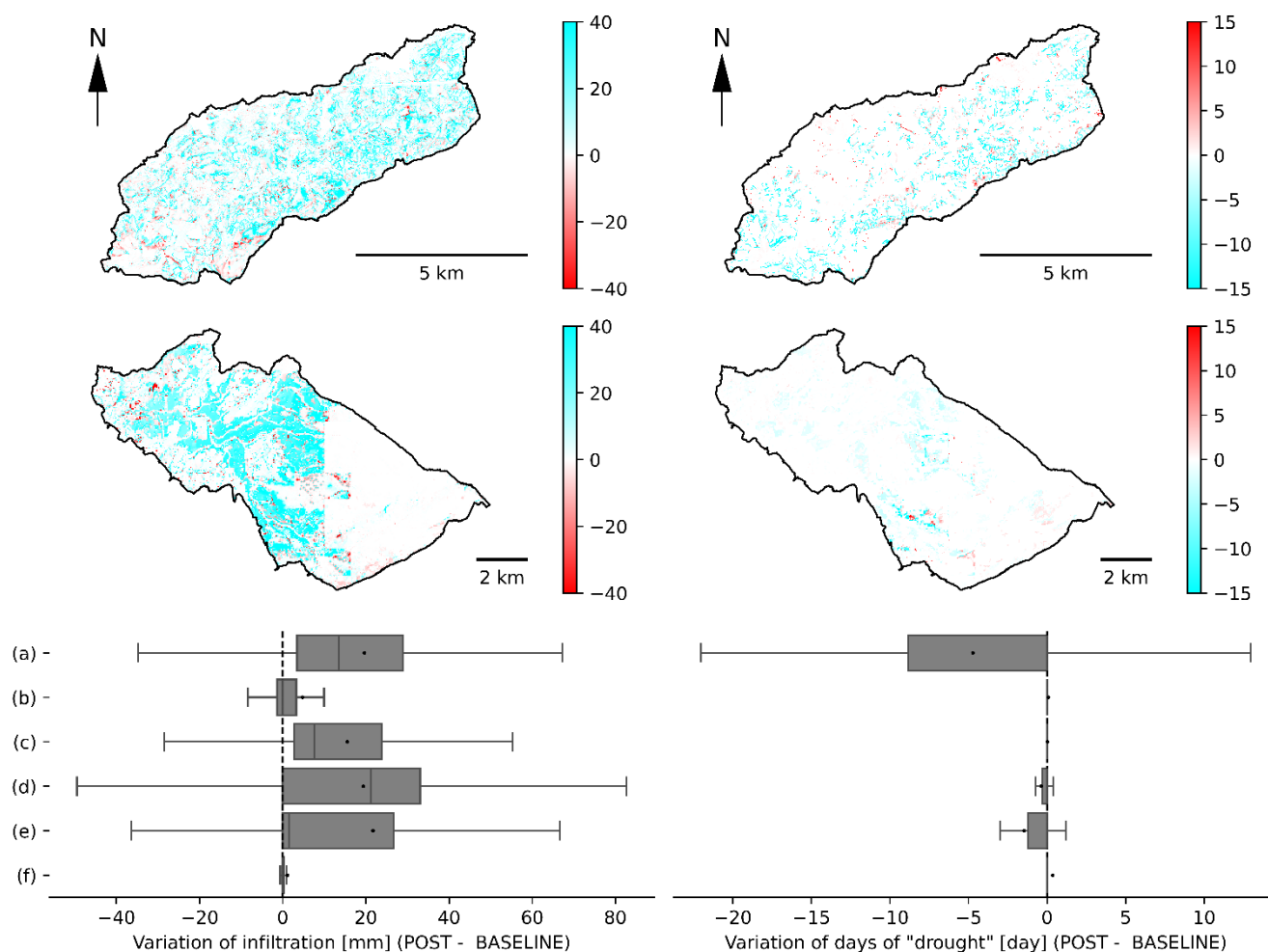
330

3.3 Effectiveness of individual NbS in mitigating floods and agricultural droughts

The following sections explore the effectiveness of individual measures. To this end, the analysis focuses on the rainfall event that occurred between 13 July and 18 July 2021.



335 As highlighted in Figure 5, model outcomes indicate that NbS generally exhibit positive effects on infiltration (and runoff reduction) and the mitigation of agricultural drought. However, the magnitude of these effects seems to vary depending on the specific type of NbS and context, as observed in the previous section.



340 **Figure 5: Variation of cumulative infiltration (from 13 to 18 July 2021) and days of drought (matric potential of -30m and return period of 25 years) on model grid cells before (BASELINE) and after (POST) implementing NbS (a : Hedgerows, b : Reduced tillage, c : Soil pitting, d : Forest practices aimed at limiting soil compaction, e : Forest diversification with practices aimed at limiting soil compaction, f : Restoration of peatlands).**

3.3.1 Hedgerows

345 In the agricultural context (Figure 5-a), hedgerows were found to be highly effective in improving infiltration during an extreme rainfall event, as reviewed by Rajbanshi et al. (2023). This modelled increase in infiltration during extreme events can be attributed to two primary factors: the enhancement of the soil's hydrodynamic properties and the generally drier soil conditions under hedgerows, which increases the unfilled soil porosity and the hydraulic gradient responsible for infiltration.



Due to the lack of farm traffic, greater incorporation of organic matter, or root network promoting macropores, soils under hedgerows are found to be less compacted and more permeable than those in adjacent arable or pasture fields (Holden et al., 2019; Wallace et al., 2021). Drier soil conditions under hedgerows can be attributed to increased actual evapotranspiration (Benhamou et al., 2013) and canopy interception. A counterintuitive observation from our simulations is that, when considering a broader temporal window, the cumulative annual modelled infiltration decreased under hedgerows due to this increased canopy interception; a larger portion of the rainfall was directly evaporated before reaching the soil for smaller and more common events (results not shown). Hedgerows have also been modelled to reduce agricultural droughts, as their root systems extend deeper than those of crops or meadows (Table 1). This allows them to access water in deeper and wetter soils layers even though soils in surface were generally drier.

3.3.2 Agricultural practices

Soil pitting in maize crop was also effective in enhancing modelled infiltration during extreme rainfall events (Figure 5-c), as observed by Clement et al. (2023). However, model outcomes showed a minimal effect of soil pitting on agricultural drought mitigation. This may suggest that extreme rainfall events, when a surplus of infiltration is observed, may be temporally disconnected from droughts events: so, they do not follow close enough together in time for the excess infiltrated water to remain in the root zone until the agricultural drought begins. Another potential factor could be the implementation of hedgerows along field margins in the same scenario, drying soils at the edges and negatively affecting water availability for adjacent crops (Forman and Baudry, 1984).

For reduced tillage practices (Figure 5-b), we did not model large changes in infiltration during extreme events, as reviewed by Clement et al. (2024), nor did we model mitigation of agricultural drought. A well-known positive effect of conservation tillage is the concentration of organic matter into the uppermost soil layer (Haddaway et al., 2017), improving in turn aggregate formation (Chen et al., 2020; Obalum et al., 2019), pore size distribution and soil water retention characteristics (Chandrasekhar et al., 2019). In our model scenario, reduced tillage was virtually implemented by reducing the Van Genuchten alpha parameter of the topsoil by 20 %. This adjustment slightly shifted the soil porosity towards smaller pores, specifically from the range of 0 to -330 hPa to the range of -330 hPa to -15000 hPa, consequently increasing the soil's available water holding capacity. Despite expectations that this improvement in soil physical quality would buffer agricultural drought, our simulation results showed no significant positive effect on mitigating it. Wittwer et al. (2023) recently suggested that while conservation tillage practices could improve soil characteristics, they do not significantly affect root water uptake patterns under severe drought conditions. Moreover, they emphasized that plant ecophysiology and cropping system diversification in space (crop mixture) and time (crop rotation) (Sanford et al., 2021) have a greater impact on crop performance under drought than soil quality. This is a conclusion that our simulation results seem to support. NbS that were modelled to solely improve the retention characteristics of surface soils without affecting root depth, such as reduced tillage practices or even forest practices aimed at limiting soil compaction, had a minimal effect on reducing vegetation water stress. One possibility is, during dry periods, soil desiccates from the surface downward over time.



Therefore, if the plant root system extends deeper than the surface soil layer, enhancing the retention properties of this superficial layer, where desiccation occurs first, does not seem to be very impactful for increasing plant resilience to prolonged droughts.

3.3.3 Forest practices

385 In the forest context, forest diversification was found to be effective in improving infiltration during extreme rainfall events and decreasing days of agricultural droughts (Figure 5-e). Mixed forests are often shown to outperform monocultures regarding agricultural drought resistance, especially in dry areas (Liu et al., 2022; Pardos et al., 2021). In our model scenario, forest diversification was implemented primarily by increasing rooting depth, reflecting the observation that mixed forests often develop deeper and more structurally developed root systems than monocultures, especially spruce even-aged
390 plantations that are common in the C2. This results from the inherent differences in rooting patterns between species, leading to generally deeper root extensions or denser fine root systems in mixed stands compared to pure stands (Jose et al., 2006; Meinen et al., 2009), as well as from the competitive environment in mixed stands, which may encourage greater root investment (Reubens et al., 2007). However, the drought resilience of mixed forests may also be attributed to other mechanisms, such as resource partitioning (e.g., root stratification), facilitation (e.g., active hydraulic redistribution), and
395 selection (e.g., a higher likelihood of including drought-tolerant species) (Pardos et al., 2021). However, these complex mechanisms were not explicitly represented in the model.

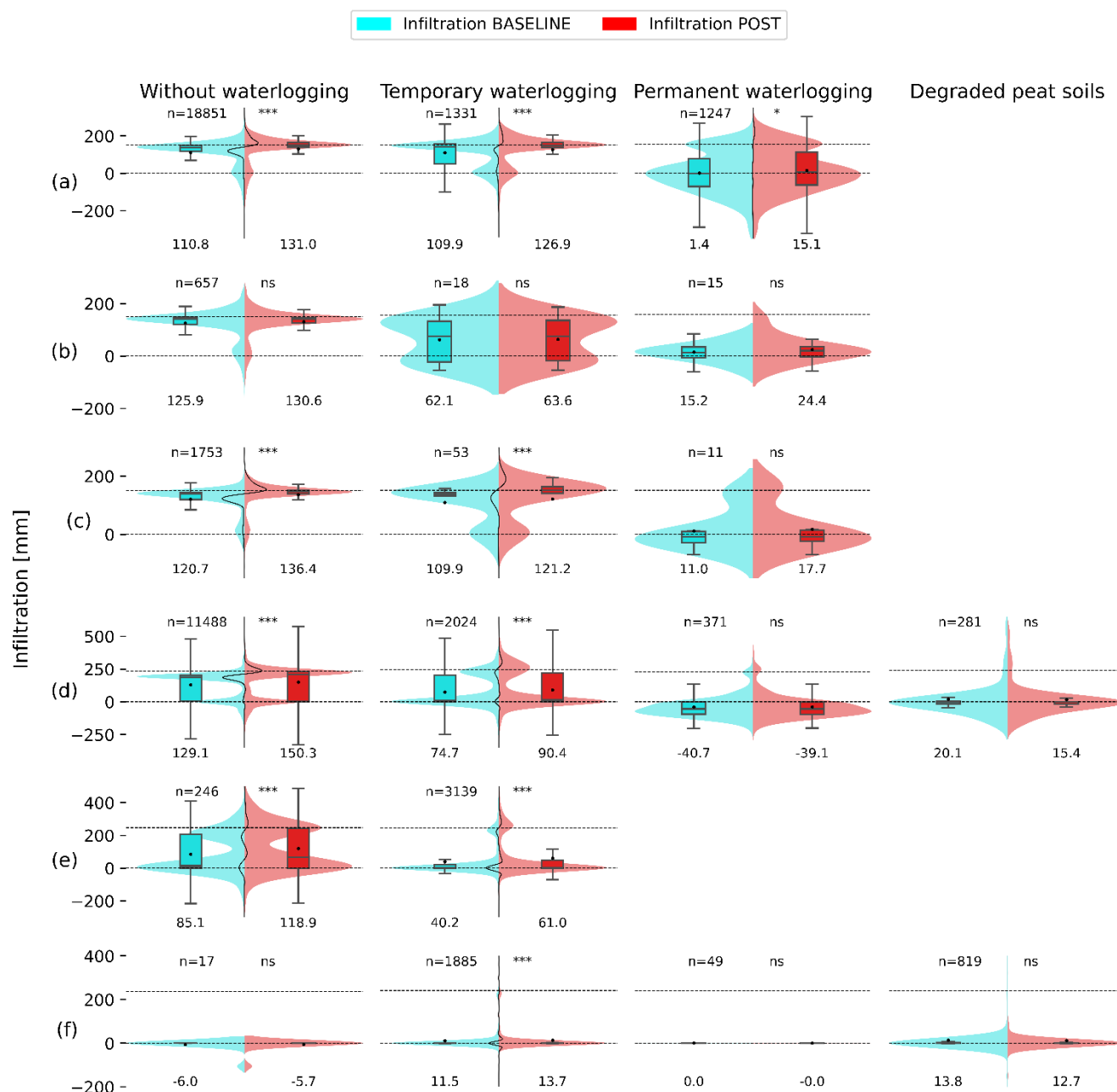
Practices aimed at limiting forest soil compaction (Figure 5-d) were also found to be effective in improving infiltration but exhibited low efficiency in reducing agricultural drought, as rooting depth was not increased with this measure.

In accordance with the current literature (Wastiaux, 2008), our model showed almost no improvement of infiltration and
400 agricultural drought mitigation after peatland restoration in moors or in drained spruce plantations on degraded peat soil (Figure 5-f).

3.4 Spatial variability of effectiveness of NbS against flood

This section examines spatial variability and the role of soil characteristics in the effectiveness of modelled NbS against floods, with the aim of identifying the most effective NbS-location combinations. The displayed cumulative infiltration data
405 from 13 to 18 July 2021, before (BASELINE) and after (POST) implementing NbS, are modelled for each natural drainage class (Table 2) from the Belgian soil map (Figure 6). Almost all infiltration distributions exhibited a characteristic bimodal shape: one peak near zero, where the soils do not or barely infiltrate, and another peak where infiltration approaches the total cumulative rainfall. Based on these distributions, we can identify runoff production zones (below the cumulative precipitation) and runoff interception/reinfiltration zones (above). Grid cells with negative infiltration rates indicate areas
410 where seepage flow is occurring.

Observing the density distributions of infiltration, a shift is evident between non-saturated soils and more saturated soils, with soils without waterlogging generally exhibiting higher infiltration rates than waterlogged soils.



415 **Figure 6: Comparison of cumulative infiltration (from 13 to 18 July 2021) before (BASELINE) and after (POST) implementing**
NbS (a : Hedgerows, b : Reduced tillage, c : Soil pitting, d : Forest practices aimed at limiting soil compaction, e : Forest
diversification with practices aimed at limiting soil compaction, f : Restoration of peatlands) for each drainage classes from the
Belgian soil map. Each data points (n) represent the infiltration of one model grid cell. Significance levels - ns (p-value>0.05), *
(0.01<p-value<0.05), ** (0.001<p-value<0.01), * (p-value<0.001) - indicate results of Kolmogorov-Smirnov tests comparing**
BASELINE and POST distributions. The centred vertical black lines depict the difference in kernel density estimates between
different BASELINE and POST distributions. Numbers below each boxplot and black points are the means. Horizontal dotted
lines represent 0 infiltration and mean cumulated rainfall between 13 and 18 July 2021.
 420



When comparing the BASELINE and POST infiltration distributions and their significance levels, it becomes clear that the effectiveness of NbS in enhancing infiltration diminishes as soil water saturation increases. This trend is observed across a gradient from well-drained soils to temporarily waterlogged areas, degraded peat soils, and permanently waterlogged zones. These findings suggest that well-drained soils offer greater potential for improving infiltration, indicating that investments should prioritize these areas for maximizing NbS effectiveness.

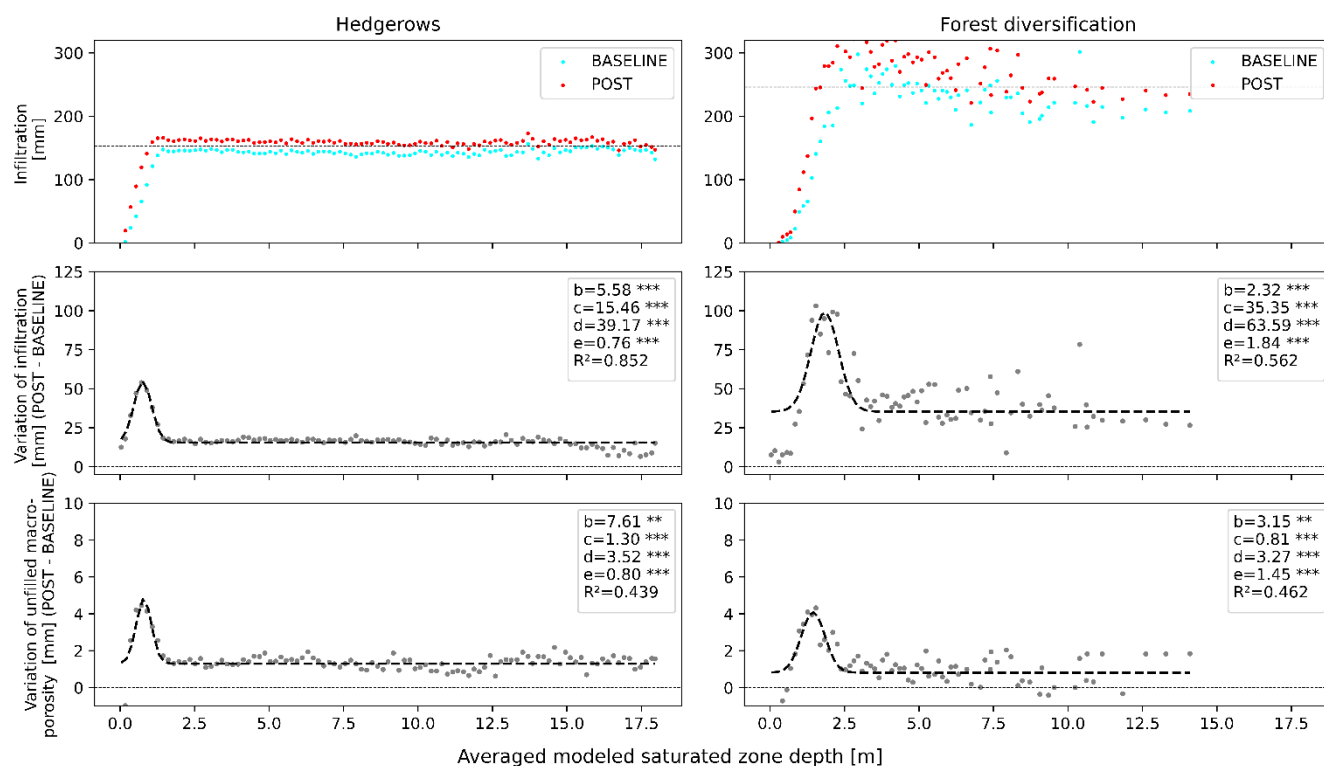
This might also explain why forest practices aimed at reducing soil compaction have been slightly more effective than forest diversification combined with these practices (Figure 5): the latter were mostly implemented on soils prone to temporary waterlogging, whereas the former were predominantly applied to well-drained soils (Figure 6). In waterlogged soils, the enhanced permeability at the surface did not result in increased infiltration rates because the soil was saturated or close to saturation.

Conversely, in the absence of waterlogging constraints, enhancing soil surface properties significantly increased infiltration. This effect was further amplified by changes in initial soil moisture conditions before rainfall events, as seen in the cases of hedgerows and forest diversification (Figure 7). The transition to more evaporative vegetation generally leads to drier surface soils locally. This drying reduces the shallow soil water matric potential, thereby increasing the hydraulic gradient responsible for infiltration. However, the magnitude of this effect on the variation of initial moisture conditions is not uniformly distributed within the watershed, and seems to vary with soils' natural drainage, or averaged saturated zone depth (Figure 7).

In areas where soils are permanently or temporarily waterlogged, the implementation of hedgerows or forest diversification did not affect initial soil moisture conditions or had only a minimal effect. This may be due to the anoxic conditions that might limit root development and transpiration (Caubel, 2001). Additionally, in these areas, increased evapotranspiration may not result in drier soils, as water consistently flows towards these areas from adjacent waterlogged soils.

In initially dry soils, increased evapotranspiration results in somewhat drier soil conditions, but the effect on enhanced infiltration is moderate. The reason for this is that the modelled infiltration capacity of these soils was barely surpassed by rainfall intensity on the extreme event of July 2021 (Figure 7).

In contrast, soils with an average groundwater table depth between 0.5 m and 2 m exhibit optimal conditions for improving infiltration, as evidenced by a significant bell-shaped function (Figure 7). In these areas, increased evaporation enhances unfilled soil macroporosity, also represented by a bell-shaped function (Figure 7). The resulting increased pore space, coupled with a higher hydraulic gradient, significantly boosted infiltration. These soils corresponded to soils without waterlogging with moderate or imperfect drainage, in the Belgian soil classification. Our findings suggest that such areas are the most favorable for implementing NbS that enhance evapotranspiration, such as hedgerows, to improve infiltration within a watershed.



455 **Figure 7: Impact of hedgerows and forest diversification on infiltration and antecedent soil moisture conditions as function of the**
average saturated zone depth. Top: Cumulative infiltration from 13 to 18 July 2021. The horizontal line is the spatially averaged
cumulated rainfall. Middle: Variation of cumulative infiltration from 13 to 18 July 2021. Bottom: Variation of unfilled
macroporosity (porosity defined between 0 and -100 cm of matric potential) in the top 30 cm of soil on 12 July 2021. The abscissa is
the average modelled saturated zone depth (from 1 January 2004 to 31 December 2021). Data points represent average
 460 **observations for fixed saturated zone depth intervals. The dotted line represents a non-linear bell-shaped regression (Bragg : $y =$**
 $c + (d \exp(-b(x-e)^2))$) fitted to observed data where : b is the slope around the inflection points of the bell, c is the constant
adjusting the minimum, d+c is the maximum value at the top of the bell and e is the x value at which such maximum occurs.

Additionally, in soils without waterlogging, reinfiltration (also called runon) of runoff generated uphill can occur. This
 phenomenon is clearly illustrated in Figure 6, where infiltration rates exceed precipitation rates. Typically, runoff-runon
 465 processes occur where areas of low infiltration capacity lie upslope of areas with higher infiltration capacity (Woolhiser et
 al., 1996). Hence, runoff-runon processes highly depend on the spatial heterogeneity of soil infiltration capacity. In our
 simulations, runoff-runon processes mostly coincide with areas with good infiltration capacity just downstream of
 impermeabilized soils, such as roads or urbanized zones. These areas, we believe, should be prioritized when implementing
 NbS that aim at retaining overland runoff and optimizing reinfiltration and evapotranspiration, such as retention ponds, rain
 470 gardens, or keylines. However, further research would be needed to confirm these findings.

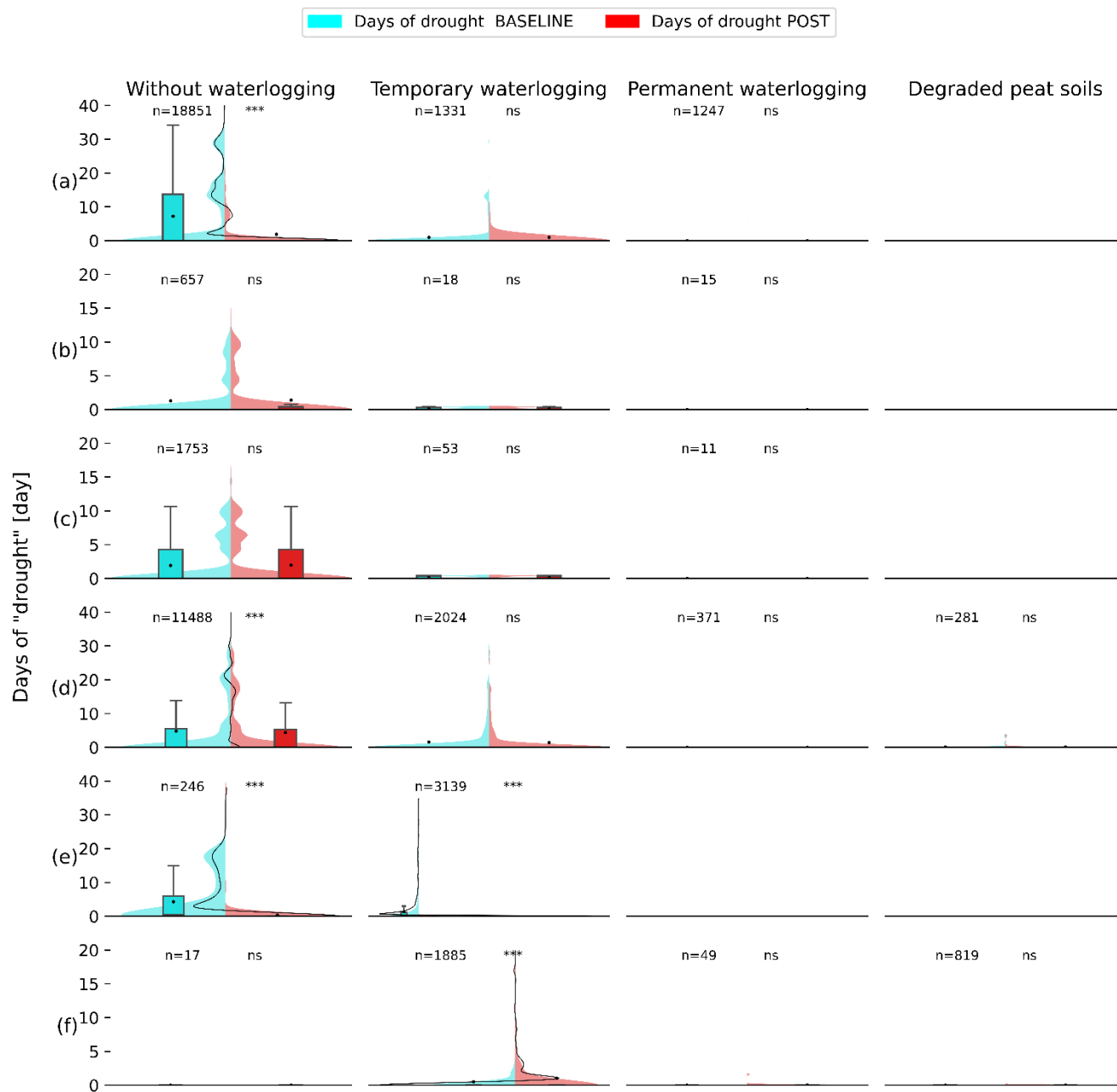


Figure 8: Comparison of days of drought (matric potential of -30m and return period of 25 years) before (BASELINE) and after (POST) implementing NBS (a : Hedgerows, b : Reduced tillage, c : Soil pitting, d : Forest practices aimed at limiting soil compaction, e : Forest diversification with practices aimed at limiting soil compaction, f : Restoration of peatlands) for each drainage classification from the Belgian soil map. Each data points (n) represent the infiltration of one model grid cell. Significance levels - ns (p-value>0.05), * (0.01<p-value<0.05), ** (0.001<p-value<0.01), *** (p-value<0.001) - indicate results of Kolmogorov-Smirnov tests comparing BASELINE and POST distributions. The centred vertical black lines depict the difference in kernel density estimates between different BASELINE and POST distributions.

475



3.5 Spatial variability of effectiveness of NbS against agricultural drought

480 The density distributions of days experiencing vegetation stress across different soil drainage classes reveal that such stresses
are most prevalent in soils without waterlogging (Figure 8). The vegetation in temporarily waterlogged areas, degraded peat
soils, and permanently waterlogged zones was far less susceptible to these stresses, primarily due to the naturally higher soil
water availability in these environments, even after prolonged droughts. Therefore, NbS installed on non-waterlogged/water
limited soils were the most effective in limiting agricultural drought. As a concrete example, hedgerows implemented on
485 temporarily waterlogged soils showed a limited effect on drought compared to soils without waterlogging (Figure 8–a).

3.6 Synergies and trade-offs between flood and drought mitigation with NbS

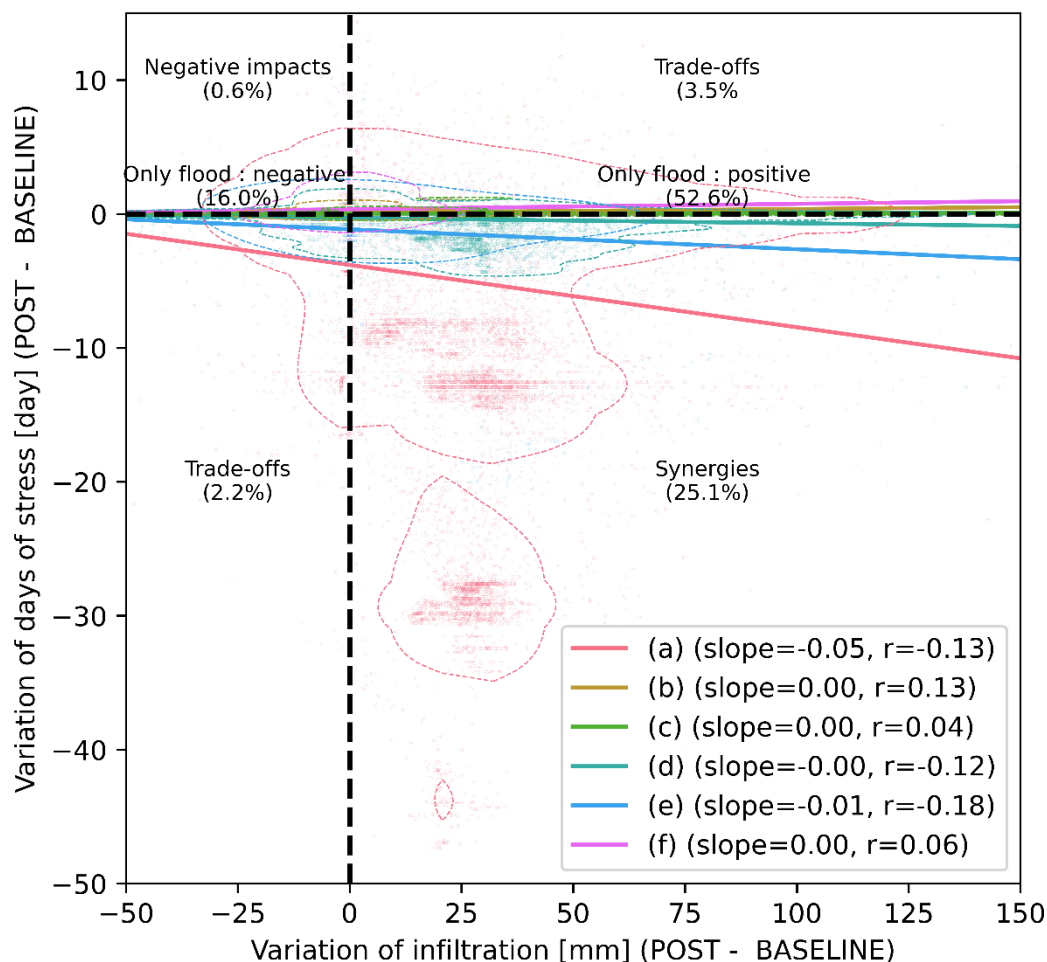
The tested NbS primarily had a positive impact on flood reduction with 80.6 % of managed grid cells showing improved
infiltration capacity (Figure 9). In contrast, the positive impact on agricultural drought was less significant, with only 27.3 %
of managed grid cells exhibiting improvement. However, we observed a minimal negative impact from NbS on agricultural
490 droughts, with only 4.1 % of managed grid cells being affected. In most cases (68.6 % of managed grid cells), there was no
discernible impact of NbS on agricultural droughts.

Managed grid cells that were positively affected against both floods and agricultural droughts (25.1 %) were predominantly
those with hedgerows and forest diversifications (Figure 9). Nevertheless, we believe that the observed relationship between
increased infiltration during extreme rainfall events and reduced vegetation water stress is not causal, but just correlated.
495 This correlation may be primarily explained by changes in vegetation and modelled root depth (Table 1 and Table 3), rather
than by an increase in infiltration. Notably, NbS that substantially reduced the number of days experiencing water stress,
such as hedgerows or forest diversification combined with practices aimed at limiting soil compaction, also resulted in drier
soils due to higher initial interception and evapotranspiration rates. However, a common characteristic of these NbS is the
modification of the vegetation and, consequently, root depth, counterbalancing drier upper soil layers. Increased root depth
500 benefits against agricultural drought in two primary ways: it expands the volume of soil reachable to roots, thereby
increasing the total available water. Furthermore, deeper root systems enable plants to access deeper and typically wetter soil
layers, which can be critical during periods of prolonged drought. It has been reviewed that a deeper root system can
significantly enhance drought resistance, particularly in water limited environments where subsoil water is available (Li et
al., 2022).

505 On the other hand, the implementation of NbS that extend root depth can enhance infiltration, as an extensive root network
facilitates the formation of macropores within the soil matrix, even after root senescence (Beven and Germann, 1982;
Wallace et al., 2021). Additionally, a robust root system supports substantial water uptake to facilitate transpiration, which
consequently leads to soil drying (Caubel, 2001). Soil desiccation promotes infiltration by increasing the hydraulic gradient
between surface and soil, by creating more air filled spaces for water to infiltrate, and by inducing structural cracks that



510 facilitate rapid preferential flow (Zhu et al., 2018). However, this very specific phenomenon was not represented in the model.



515 **Figure 9: Scatter plot and regression lines of the variation cumulative infiltration (from 13 to 18 July 2021) against days of drought (matric potential of -30m and return period of 25 years) on model grid cells before (BASELINE) and after (POST) implementing NbS (a : Hedgerows, b : Reduced tillage, c : Soil pitting, d : Forest practices aimed at limiting soil compaction, e : Forest diversification with practices aimed at limiting soil compaction, f : Restoration of peatlands). Vertical and horizontal lines represent thresholds between negative and positive impacts on flood and drought, respectively. Percentages represent the proportion of total points (model grid cells) inside and between each quadrant.**

520 From this perspective, promoting root growth and sustaining plant transpiration could be considered important to help reduce both vegetation water stress, caused by prolonged drought, and flood risks. In an agricultural context, this can be achieved by limiting soil compaction, which might also hamper infiltration (Unger and Kaspar, 1994). For instance, biopores have been found to substantially mitigate transpiration deficits during droughts by promoting root systems as preferential growth paths permitting crops to access water from deeper and moister soil layers (Landl et al., 2019). Compaction caused by machinery



525 traffic in forest soils may also reduce the rooting density of trees due to a lack of soil aeration (von Wilpert and Schäffer, 2006) and an increased ground penetration resistance (Goutal, 2012).

Finally, it is important to note that the balance between synergies and trade-offs is not solely dependent on the type of NbS but also on the location where they are implemented. As discussed in previous sections, NbS were more effective in soils without waterlogging, both in mitigating the risks of flooding and addressing agricultural droughts.

530 **3.7 Study limitations and knowledge gaps**

Representing the hydrological functioning of a watershed at a fine spatial scale remains a challenge for modellers. Indeed, physically based distributed hydrological models require a large number of parameters to be determined or calibrated. However, the data required for model calibration and validation are often unavailable or highly uncertain at the necessary scale. For instance, calibrating and validating models at the watershed outlet does not necessarily ensure accurate
535 representation of the spatialized hydrological processes within the watershed. Multiple combinations of spatialized model input parameters can yield identical modelled hydrographs at the catchment outlet. Nonetheless, a semi-quantitative spatial validation was made by comparing the spatially distributed average depths of the modelled saturated zone with the drainage classes from the Belgian soil map. Although it is an interesting approach, since this map is specific to Belgium, it is not directly transposable to other regions. This calls for future research on spatially distributed and cross-scale hydrological
540 observations to calibrate and validate models.

The results indicated that soil infiltration capacity is a crucial factor in determining the most suitable locations for implementing NbS. However, accurately representing the spatial and temporal (Pirlot et al., 2024) variability of soil hydrodynamic properties remains challenging with current methodologies. The maps depicting the soils hydrodynamic properties are inherently limited in their representativeness due to uncertainties in the applied pedotransfer functions, which
545 are primarily derived from agricultural soils, overlooking much of the soil diversity, such as stony soils. Additional limitations arise from uncertainties and the spatial resolution of the underlying soil property maps (e.g., soil depth, texture, organic carbon, and bulk density), as well as the suitability of the continuous function used to describe soil hydrodynamic properties (Weber et al., 2024).

Similarly, vegetation plays a crucial role in the soil hydrological functioning at fine scales, significantly influencing
550 watersheds dynamics. A striking example is the impact of planting hedgerows, which locally decreases soil moisture, enhancing infiltration rates, resulting in substantial reductions in peak flow at the watershed outlet. However, the understanding of vegetation characteristics (also used as model input), particularly tree rooting systems, remains surprisingly underdeveloped. Despite their critical role, our understanding of roots, including their growth, development, and interaction with complex physical, chemical, and biological soil properties, is still limited (Centenaro et al., 2018).

555 In the present article, the potential synergies or trade-offs that can arise with NbS for mitigating floods and agricultural droughts were evaluated. These types of findings can later be incorporated into cost-benefit analyses, providing justification for or against specific actions (e.g. Fennell et al., 2023b). However, other co-benefits or trade-offs may emerge, which



should be assessed according to the specific context and interests of the region in question. For example, afforestation is known to increase watershed evapotranspiration, reducing river flow and groundwater levels. While this trade-off may be limited in humid climates (Hou et al., 2023; Zhang et al., 2017), which are also less prone to hydrological droughts, such practices, like planting alien trees, could be problematic in arid or semi-arid regions that are more sensitive to long term hydrological and socio-economic droughts (Rebelo et al., 2022). Hence the impacts of these actions extend beyond hydrological effects, encompassing important social, cultural, economic, and environmental aspects (Sowińska-Świerkosz and García, 2021), which may not all be quantifiable in financial terms. NbS are inherently integrative and multifunctional; focusing solely on a hydrological performance without considering the broader social, economic, political (governance) and environmental context can undermine the success and legitimacy of projects (Brauman et al., 2022).

It should be noted that the proposed "infiltration" indicator may not be a sufficient measure of the effectiveness of a NbS in reducing flood risks. This indicator only assesses the effectiveness of NbS in mitigating the hazard itself and does not recognize downstream exposure or vulnerability, which are crucial factors to consider when planning flood risks management (Klijn et al., 2015). For a comprehensive assessment of the effectiveness of NbS it is crucial to adopt cross-scale approaches since the effects of NbS are not necessarily confined to the immediate area of implementation. For example, interventions may reduce flood risks locally, but their impacts can also be felt much farther downstream (Lane, 2017). Similarly, tree planting, while potentially increasing local hydrologic drought risk due to higher evapotranspiration rates, may provide benefits on a larger scale through recycling of atmospheric moisture (Keys et al., 2018; Theeuwens et al., 2023). These dynamics demonstrate that the evaluation of NbS cannot be conducted in isolation; it requires models capable of capturing complex interactions across scales and processes, representing the frontiers of the current science.

Currently, there is no globally accepted or standardized approach for monitoring NbS (Kumar et al., 2021). The fine-scale spatial variability of effectiveness of NbS raise important questions regarding the appropriate methods and scales for monitoring these interventions after implementation. These approaches should be determined based on the type, extent, and expected outcomes of NbS. Macro-scale indicators at the watershed level, such as reductions in peak flow, can be highly useful for assessing the overall, cumulative effects of a series of NbS implemented upstream. However, such indicators do not distinguish the individual impacts of specific interventions. Therefore, fine-scale indicators are also necessary to optimize the benefits of NbS. Nevertheless, these assume that individual interventions act independently and do not interact at small scales, an assumption that may not be always true. Also, monitoring approaches often rely on ground-based measurement stations, that are limited in number and scattered sparsely. Recent advances in airborne and satellite-based remote sensing technologies have enabled the possibility to bridge this gap between scales, improving the capacity to systematically monitor NbS performance (Kumar et al., 2021). For instance, monitoring the effectiveness of NbS in mitigating agricultural drought can be achieved through the comparison of vegetation indices such as the Normalized Difference Vegetation Index (NDVI) or the Vegetation Health Index (Patel et al., 2012). Flood and estimated damage costs might also be evaluated by GIS-based monitoring (Haq et al., 2012).

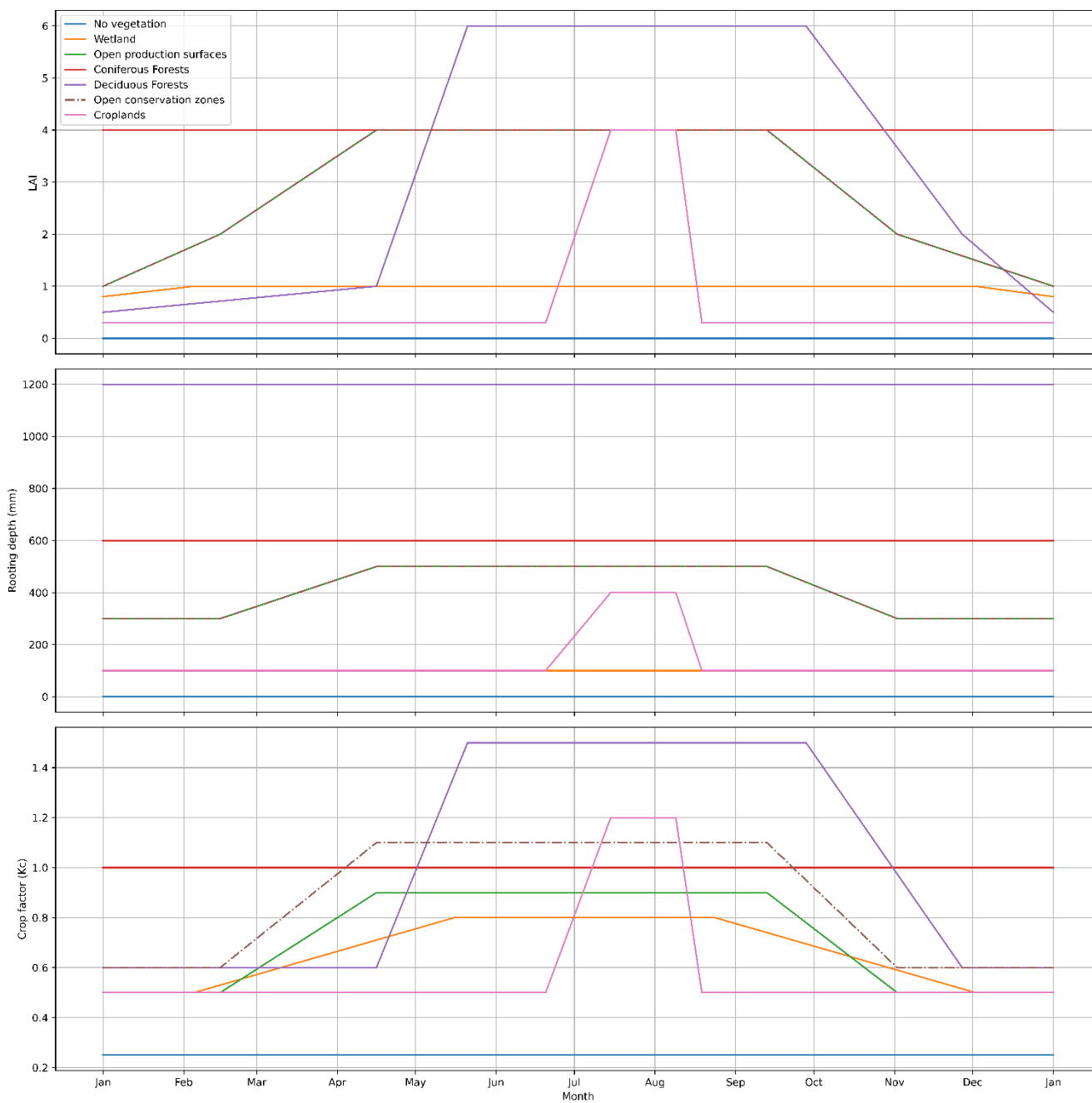


4 Conclusion

We presented a method, with innovative indicators, to evaluate the effectiveness of NbS implemented in productive forests and agricultural catchments for flood and agricultural drought mitigation. Our results emphasized the critical role of spatial variability in NbS effectiveness, influenced by soil characteristics. A key finding is that the effectiveness of NbS in reducing flood risk is significantly influenced by the soil's natural drainage characteristics, which vary across a watershed. In this study, soils with moderate drainage characteristics exhibited the highest potential for enhanced infiltration through NbS that increase evapotranspiration, such as hedgerows. Additionally, NbS that enhanced root depth were most effective in mitigating agricultural drought, especially in water-limited environments. The study, finally, acknowledges the challenges of current modelling and monitoring techniques, particularly in the importance of accurately capturing soil hydrodynamic and vegetation behaviours affecting small-scale NbS performance. Overall, these findings underscore the necessity for context specific and cross-scales assessments of NbS, considering trade-offs and co-benefits in both environmental and socio-economic spheres.



Appendix A



605 Figure - A1: Vegetation development trajectories (LAI, rooting depth and Kc) used as model input to calculate evapotranspiration.



Code and data availability

Most input data are open source and are cited in the article. MIKE SHE/MIKE 1D is proprietary software. Model output data and codes that support the findings of this study are available upon request.

Author contributions

610 BG: Conceptualization; Data curation; Formal analysis; Investigation; Software; Methodology; Visualization; Writing – original draft preparation; Writing – review & editing.

AM: Conceptualization; Data curation; Formal analysis; Investigation; Software; Methodology; Writing – review & editing.

AD: Conceptualization; Methodology; Project administration; Supervision; Funding acquisition; Writing – review & editing.

Competing interests

615 The authors declare that they have no conflict of interest.

Acknowledgements

We thank Noémie Bonaventure, Lisa Di Maggio, Emmanuelle Leyh, and Sara Rabouli for their active participation in the “ModRec Vesdre” project. We also give credit to the Studio023PaolaViganò team (Milan, Bruxelles) and Jacques Teller's team (Uliège) for their contributions to the “Schéma stratégique multidisciplinaire du bassin versant de la Vesdre”

620 (<https://territoire.wallonie.be/fr/page/inondations>), which was used in this study to develop landscape planning scenarios.

Financial support

This study was conducted as part of the “ModRec Vesdre” agreement (<https://orbi.uliege.be/handle/2268/314437>), funded by the SPW Agriculture, ressources naturelles et Environnement (D GARNE).

References

625 Aalbers, E. E., van Meijgaard, E., Lenderink, G., de Vries, H., and van den Hurk, B. J. J. M.: The 2018 west-central European drought projected in a warmer climate: how much drier can it get?, *Natural Hazards and Earth System Sciences*, 23, 1921–1946, <https://doi.org/10.5194/nhess-23-1921-2023>, 2023.

Allan, R., Pereira, L., and Smith, M.: *Crop evapotranspiration-Guidelines for computing crop water requirements-FAO Irrigation and drainage paper 56*, 1998.



- 630 Carte Numérique des Sols de Wallonie: <https://metawal.wallonie.be/geonetwork/srv/fre/catalog.search#/metadata/c5bedf2b-1cac-4231-9d9a-854e0ef2c9ce>, last access: 9 August 2024a.
- Carte Numérique des Sols de Wallonie: <https://metawal.wallonie.be/geonetwork/geoportailwal/fre/catalog.search#/metadata/38c2a87e-d38a-4359-9899-9d4a6b9f0c2a>, last access: 14 November 2023b.
- 635 Gridded observational data: https://opendata.meteo.be/geonetwork/srv/eng/catalog.search#/metadata/RMI_DATASET_GRIDDEDOBS.
- Textures et fractions granulométriques de référence des sols de Wallonie - Série: <https://metawal.wallonie.be/geonetwork/geoportailwal/fre/catalog.search#/metadata/e90eb7cf-8f7d-40ab-9df9-5c34ddf387ea>, last access: 13 November 2023.
- 640 Bassine, C., Radoux, J., Beaumont, B., Grippa, T., Lennert, M., Champagne, C., De Vroey, M., Martinet, A., Bouchez, O., Deffense, N., Hallot, E., Wolff, E., and Defourny, P.: First 1-M Resolution Land Cover Map Labeling the Overlap in the 3rd Dimension: The 2018 Map for Wallonia, *Data*, 5, 117, <https://doi.org/10.3390/data5040117>, 2020.
- Bathurst, J. C., Fahey, B., Iroumé, A., and Jones, J.: Forests and floods: Using field evidence to reconcile analysis methods, *Hydrological Processes*, 34, 3295–3310, <https://doi.org/10.1002/hyp.13802>, 2020.
- 645 Benhamou, C., Salmon-Monviola, J., Durand, P., Grimaldi, C., and Merot, Ph.: Modeling the interaction between fields and a surrounding hedgerow network and its impact on water and nitrogen flows of a small watershed, *Agricultural Water Management*, 121, 62–72, <https://doi.org/10.1016/j.agwat.2013.01.004>, 2013.
- Beven, K. and Germann, P.: Macropores and water flow in soils, *Water Resources Research*, 18, 1311–1325, <https://doi.org/10.1029/WR018i005p01311>, 1982.
- 650 Brauman, K. A., Bremer, L. L., Hamel, P., Ochoa-Tocachi, B. F., Roman-Dañobeytia, F., Bonnesoeur, V., Arapa, E., and Gammie, G.: Producing valuable information from hydrologic models of nature-based solutions for water, *Integrated Environmental Assessment and Management*, 18, 135–147, <https://doi.org/10.1002/ieam.4511>, 2022.
- Cammalleri, C., Naumann, G., Mentaschi, L., Formetta, G., Forzieri, G., Gosling, S., Bisselink, B., De Roo, A., and Feyen, L.: Global warming and drought impacts in the EU, Publications Office of the European Union, 2020.
- 655 Caubel, V.: Influence de la haie de ceinture de fond de vallée sur le transfert d'eau et de nitrate, These de doctorat, Rennes, ENSA, 2001.
- Centenaro, G., Hudek, C., Zanella, A., and Crivellaro, A.: Root-soil physical and biotic interactions with a focus on tree root systems: A review, *Applied Soil Ecology*, 123, 318–327, <https://doi.org/10.1016/j.apsoil.2017.09.017>, 2018.
- Chandrasekhar, P., Kieselmeier, J., Schwen, A., Weninger, T., Julich, S., Feger, K.-H., and Schwärzel, K.: Modeling the evolution of soil structural pore space in agricultural soils following tillage, *Geoderma*, 353, 401–414, <https://doi.org/10.1016/j.geoderma.2019.07.017>, 2019.
- Chen, H., Dai, Z., Veach, A. M., Zheng, J., Xu, J., and Schadt, C. W.: Global meta-analyses show that conservation tillage practices promote soil fungal and bacterial biomass, *Agriculture, Ecosystems & Environment*, 293, 106841, <https://doi.org/10.1016/j.agee.2020.106841>, 2020.



- 665 Clement, T., Bielders, C. L., Degré, A., Manssens, G., and Foucart, G.: Soil pitting mitigates runoff, erosion and pesticide surface losses in maize crops in the Belgian loess belt, *Soil and Tillage Research*, 234, 105853, <https://doi.org/10.1016/j.still.2023.105853>, 2023.
- Clement, T., Bielders, C. L., and Degré, A.: How much do conservation cropping practices mitigate runoff and soil erosion under Western European conditions: A focus on conservation tillage, tied ridging and winter cover crops, *Soil Use and Management*, 40, e13047, <https://doi.org/10.1111/sum.13047>, 2024.
- 670
- DHI: MIKE SHE User Guide and Reference Manual, 2024.
- Ditzler, C.: A Glossary of Terms Used in Soil Survey and Soil Classification, Soil Taxonomy | Natural Resources Conservation Service, 1999.
- Dottori, F., Mentaschi, L., Bianchi, A., Alfieri, L., and Feyen, L.: Cost-effective adaptation strategies to rising river flood risk in Europe, *Nat. Clim. Chang.*, 13, 196–202, <https://doi.org/10.1038/s41558-022-01540-0>, 2023.
- 675
- Fennell, J., Soulsby, C., Wilkinson, M. E., Daalmans, R., and Geris, J.: Assessing the role of location and scale of Nature Based Solutions for the enhancement of low flows, *International Journal of River Basin Management*, 21, 743–758, <https://doi.org/10.1080/15715124.2022.2092490>, 2023a.
- Fennell, J., Soulsby, C., Wilkinson, M. E., Daalmans, R., and Geris, J.: Time variable effectiveness and cost-benefits of different nature-based solution types and design for drought and flood management, *Nature-Based Solutions*, 3, 100050, <https://doi.org/10.1016/j.nbsj.2023.100050>, 2023b.
- 680
- Forman, R. T. T. and Baudry, J.: Hedgerows and hedgerow networks in landscape ecology, *Environmental Management*, 8, 495–510, <https://doi.org/10.1007/BF01871575>, 1984.
- Gourlez de la Motte, L., Beauclaire, Q., Heinesch, B., Cuntz, M., Foltýnová, L., Šigut, L., Kowalska, N., Manca, G., Ballarin, I. G., Vincke, C., Roland, M., Ibrom, A., Lousteau, D., Siebicke, L., Neiryink, J., and Longdoz, B.: Non-stomatal processes reduce gross primary productivity in temperate forest ecosystems during severe edaphic drought, *Philosophical Transactions of the Royal Society B: Biological Sciences*, 375, 20190527, <https://doi.org/10.1098/rstb.2019.0527>, 2020.
- Goutal, N.: Modifications et restauration de propriétés physiques et chimiques de deux sols forestiers soumis au passage d'un engin d'exploitation, phdthesis, AgroParisTech, 2012.
- 690
- Granier, A., Reichstein, M., Bréda, N., Janssens, I. A., Falge, E., Ciais, P., Grünwald, T., Aubinet, M., Berbigier, P., Bernhofer, C., Buchmann, N., Facini, O., Grassi, G., Heinesch, B., Ilvesniemi, H., Keronen, P., Knohl, A., Köstner, B., Lagergren, F., Lindroth, A., Longdoz, B., Loustau, D., Mateus, J., Montagnani, L., Nys, C., Moors, E., Papale, D., Peiffer, M., Pilegaard, K., Pita, G., Pumpanen, J., Rambal, S., Rebmann, C., Rodrigues, A., Seufert, G., Tenhunen, J., Vesala, T., and Wang, Q.: Evidence for soil water control on carbon and water dynamics in European forests during the extremely dry year: 2003, *Agricultural and Forest Meteorology*, 143, 123–145, <https://doi.org/10.1016/j.agrformet.2006.12.004>, 2007.
- 695
- Haddaway, N. R., Hedlund, K., Jackson, L. E., Kätterer, T., Lugato, E., Thomsen, I. K., Jørgensen, H. B., and Isberg, P.-E.: How does tillage intensity affect soil organic carbon? A systematic review, *Environmental Evidence*, 6, 30, <https://doi.org/10.1186/s13750-017-0108-9>, 2017.
- Hallegatte, S.: Strategies to adapt to an uncertain climate change, *Global Environmental Change*, 19, 240–247, <https://doi.org/10.1016/j.gloenvcha.2008.12.003>, 2009.
- 700

Hanson, H. I., Wickenberg, B., and Alkan Olsson, J.: Working on the boundaries—How do science use and interpret the nature-based solution concept?, *Land Use Policy*, 90, 104302, <https://doi.org/10.1016/j.landusepol.2019.104302>, 2020.

705 Haq, M., Akhtar, M., Muhammad, S., Paras, S., and Rahmatullah, J.: Techniques of Remote Sensing and GIS for flood monitoring and damage assessment: A case study of Sindh province, Pakistan, *The Egyptian Journal of Remote Sensing and Space Science*, 15, 135–141, <https://doi.org/10.1016/j.ejrs.2012.07.002>, 2012.

Hari, V., Rakovec, O., Markonis, Y., Hanel, M., and Kumar, R.: Increased future occurrences of the exceptional 2018–2019 Central European drought under global warming, *Sci Rep*, 10, 12207, <https://doi.org/10.1038/s41598-020-68872-9>, 2020.

710 Holden, J., Grayson, R. P., Berdeni, D., Bird, S., Chapman, P. J., Edmondson, J. L., Firbank, L. G., Helgason, T., Hodson, M. E., Hunt, S. F. P., Jones, D. T., Lappage, M. G., Marshall-Harries, E., Nelson, M., Prendergast-Miller, M., Shaw, H., Wade, R. N., and Leake, J. R.: The role of hedgerows in soil functioning within agricultural landscapes, *Agriculture, Ecosystems & Environment*, 273, 1–12, <https://doi.org/10.1016/j.agee.2018.11.027>, 2019.

Hou, Y., Wei, X., Zhang, M., Creed, I. F., McNulty, S. G., and Ferraz, S. F. B.: A global synthesis of hydrological sensitivities to deforestation and forestation, *Forest Ecology and Management*, 529, 120718, <https://doi.org/10.1016/j.foreco.2022.120718>, 2023.

715 Jose, S., Williams, R., and Zamora, D.: Belowground ecological interactions in mixed-species forest plantations, *Forest Ecology and Management*, 233, 231–239, <https://doi.org/10.1016/j.foreco.2006.05.014>, 2006.

Journée, M., Goudenhoofd, E., Vannitsem, S., and Delobbe, L.: Quantitative rainfall analysis of the 2021 mid-July flood event in Belgium, *Hydrology and Earth System Sciences*, 27, 3169–3189, <https://doi.org/10.5194/hess-27-3169-2023>, 2023.

720 Keesstra, S., Nunes, J., Novara, A., Finger, D., Avelar, D., Kalantari, Z., and Cerdà, A.: The superior effect of nature based solutions in land management for enhancing ecosystem services, *Science of The Total Environment*, 610–611, 997–1009, <https://doi.org/10.1016/j.scitotenv.2017.08.077>, 2018.

Keys, P. W., Wang-Erlandsson, L., and Gordon, L. J.: Megacity precipitationsheds reveal tele-connected water security challenges, *PLOS ONE*, 13, e0194311, <https://doi.org/10.1371/journal.pone.0194311>, 2018.

725 Klijn, F., Kreibich, H., de Moel, H., and Penning-Rowsell, E.: Adaptive flood risk management planning based on a comprehensive flood risk conceptualisation, *Mitig Adapt Strateg Glob Change*, 20, 845–864, <https://doi.org/10.1007/s11027-015-9638-z>, 2015.

730 Kumar, P., Debele, S. E., Sahani, J., Rawat, N., Marti-Cardona, B., Alfieri, S. M., Basu, B., Basu, A. S., Bowyer, P., Charizopoulos, N., Jaakko, J., Loupis, M., Menenti, M., Mickovski, S. B., Pfeiffer, J., Pilla, F., Pröll, J., Pulvirenti, B., Rutzinger, M., Sannigrahi, S., Spyrou, C., Tuomenvirta, H., Vojinovic, Z., and Zieher, T.: An overview of monitoring methods for assessing the performance of nature-based solutions against natural hazards, *Earth-Science Reviews*, 217, 103603, <https://doi.org/10.1016/j.earscirev.2021.103603>, 2021a.

735 Kumar, P., Debele, S. E., Sahani, J., Rawat, N., Marti-Cardona, B., Alfieri, S. M., Basu, B., Basu, A. S., Bowyer, P., Charizopoulos, N., Gallotti, G., Jaakko, J., Leo, L. S., Loupis, M., Menenti, M., Mickovski, S. B., Mun, S.-J., Gonzalez-Ollauri, A., Pfeiffer, J., Pilla, F., Pröll, J., Rutzinger, M., Santo, M. A., Sannigrahi, S., Spyrou, C., Tuomenvirta, H., and Zieher, T.: Nature-based solutions efficiency evaluation against natural hazards: Modelling methods, advantages and limitations, *Science of The Total Environment*, 784, 147058, <https://doi.org/10.1016/j.scitotenv.2021.147058>, 2021b.



- Landl, M., Schnepf, A., Uteau, D., Peth, S., Athmann, M., Kautz, T., Perkons, U., Vereecken, H., and Vanderborght, J.: Modeling the Impact of Biopores on Root Growth and Root Water Uptake, *Vadose Zone Journal*, 18, 180196, <https://doi.org/10.2136/vzj2018.11.0196>, 2019.
- 740 Lane, S. N.: Natural flood management, *WIREs Water*, 4, e1211, <https://doi.org/10.1002/wat2.1211>, 2017.
- Legrain, X., Demarcin, P., Colinet, G., and Bock, L.: Cartographie des sols en Belgique : aperçu historique et présentation des travaux actuels de valorisation et de révision de la Carte Numérique des Sols de Wallonie, *Soil mapping in Belgium: historical overview and presentation of the current work on valorisation and revision of the Digital Soil Map of Wallonia*, 15, 2011.
- 745 Li, B., Zhang, X., Morita, S., Sekiya, N., Araki, H., Gu, H., Han, J., Lu, Y., and Liu, X.: Are crop deep roots always beneficial for combating drought: A review of root structure and function, regulation and phenotyping, *Agricultural Water Management*, 271, 107781, <https://doi.org/10.1016/j.agwat.2022.107781>, 2022.
- LIDAXES (version 2) - MNT: <https://metawal.wallonie.be/geonetwork/geoportailwal/api/records/346a048d-ead3-45c2-8953-fe144faa15ee>, last access: 13 November 2023.
- 750 Liu, D., Wang, T., Peñuelas, J., and Piao, S.: Drought resistance enhanced by tree species diversity in global forests, *Nat. Geosci.*, 15, 800–804, <https://doi.org/10.1038/s41561-022-01026-w>, 2022.
- Maidment, D. R.: *Handbook of hydrology*, McGraw-Hill, New York, NY, 1992.
- Meinen, C., Hertel, D., and Leuschner, C.: Biomass and morphology of fine roots in temperate broad-leaved forests differing in tree species diversity: is there evidence of below-ground overyielding?, *Oecologia*, 161, 99–111, <https://doi.org/10.1007/s00442-009-1352-7>, 2009.
- 755 Mishra, A. K. and Singh, V. P.: A review of drought concepts, *Journal of Hydrology*, 391, 202–216, <https://doi.org/10.1016/j.jhydrol.2010.07.012>, 2010.
- Moriasi, D. N., Arnold, J. G., Van Liew, M. W., Bingner, R. L., Harmel, R. D., and Veith, T. L.: Model Evaluation Guidelines for Systematic Quantification of Accuracy in Watershed Simulations, *American Society of Agricultural and Biological Engineers*, 50, 885–900, <https://doi.org/10.13031/2013.23153>, 2007.
- 760 Naumann, G., Cammalleri, C., Mentaschi, L., and Feyen, L.: Increased economic drought impacts in Europe with anthropogenic warming, *Nat. Clim. Chang.*, 11, 485–491, <https://doi.org/10.1038/s41558-021-01044-3>, 2021.
- Nesshöver, C., Assmuth, T., Irvine, K. N., Rusch, G. M., Waylen, K. A., Delbaere, B., Haase, D., Jones-Walters, L., Keune, H., Kovacs, E., Krauze, K., Külvik, M., Rey, F., van Dijk, J., Vistad, O. I., Wilkinson, M. E., and Wittmer, H.: The science, policy and practice of nature-based solutions: An interdisciplinary perspective, *Science of The Total Environment*, 579, 1215–1227, <https://doi.org/10.1016/j.scitotenv.2016.11.106>, 2017.
- 765 Obalum, S. E., Uteau-Puschmann, D., and Peth, S.: Reduced tillage and compost effects on soil aggregate stability of a silt-loam Luvisol using different aggregate stability tests, *Soil and Tillage Research*, 189, 217–228, <https://doi.org/10.1016/j.still.2019.02.002>, 2019.
- 770 Pardos, M., del Río, M., Pretzsch, H., Jactel, H., Bielak, K., Bravo, F., Brazaitis, G., Defossez, E., Engel, M., Godvod, K., Jacobs, K., Jansone, L., Jansons, A., Morin, X., Nothdurft, A., Oreti, L., Ponette, Q., Pach, M., Riofrío, J., Ruíz-Peinado, R., Tomao, A., Uhl, E., and Calama, R.: The greater resilience of mixed forests to drought mainly depends on their composition:



- Analysis along a climate gradient across Europe, *Forest Ecology and Management*, 481, 118687, <https://doi.org/10.1016/j.foreco.2020.118687>, 2021.
- 775 Patel, N. R., Parida, B. R., Venus, V., Saha, S. K., and Dadhwal, V. K.: Analysis of agricultural drought using vegetation temperature condition index (VTCI) from Terra/MODIS satellite data, *Environ Monit Assess*, 184, 7153–7163, <https://doi.org/10.1007/s10661-011-2487-7>, 2012.
- Penning, E., Burgos, R. P., Mens, M., Dahm, R., and Bruijn, K. de: Nature-based solutions for floods AND droughts AND biodiversity: Do we have sufficient proof of their functioning?, *Cambridge Prisms: Water*, 1, e11, <https://doi.org/10.1017/wat.2023.12>, 2023.
- 780 Pirlot, C., Renard, A.-C., De Clerck, C., and Degré, A.: How does soil water retention change over time? A three-year field study under several production systems, *European Journal of Soil Science*, 75, e13558, <https://doi.org/10.1111/ejss.13558>, 2024.
- Pörtner, H.-O., Roberts, D. C., Adams, H., Adelekan, I., Adler, C., Adrian, R., Aldunce, P., Ali, E., Begum, R. A., Friedl, B. B., Kerr, R. B., Biesbroek, R., Birkmann, J., Bowen, K., Caretta, M. A., Carnicer, J., Castellanos, E., Cheong, T. S., Chow, W., G. Cissé, G. C., and Ibrahim, Z. Z.: *Climate Change 2022: Impacts, Adaptation and Vulnerability*, 2022.
- Possanti, I. and Marques, G.: A modelling framework for nature-based solutions expansion planning considering the benefits to downstream urban water users, *Environmental Modelling & Software*, 152, 105381, <https://doi.org/10.1016/j.envsoft.2022.105381>, 2022.
- 790 Qiu, Y., da Silva Rocha Paz, I., Chen, F., Versini, P.-A., Schertzer, D., and Tchiguirinskaia, I.: Space variability impacts on hydrological responses of nature-based solutions and the resulting uncertainty: a case study of Guyancourt (France), *Hydrology and Earth System Sciences*, 25, 3137–3162, <https://doi.org/10.5194/hess-25-3137-2021>, 2021.
- Rajbanshi, J., Das, S., and Paul, R.: Quantification of the effects of conservation practices on surface runoff and soil erosion in croplands and their trade-off: A meta-analysis, *Science of The Total Environment*, 864, 161015, <https://doi.org/10.1016/j.scitotenv.2022.161015>, 2023.
- 795 Rebelo, A. J., Holden, P. B., Hallows, J., Eady, B., Cullis, J. D. S., Esler, K. J., and New, M. G.: The hydrological impacts of restoration: A modelling study of alien tree clearing in four mountain catchments in South Africa, *Journal of Hydrology*, 610, 127771, <https://doi.org/10.1016/j.jhydrol.2022.127771>, 2022.
- Reubens, B., Poesen, J., Danjon, F., Geudens, G., and Muys, B.: The role of fine and coarse roots in shallow slope stability and soil erosion control with a focus on root system architecture: a review, *Trees*, 21, 385–402, <https://doi.org/10.1007/s00468-007-0132-4>, 2007.
- 800 Ruangpan, L., Vojinovic, Z., Di Sabatino, S., Leo, L. S., Capobianco, V., Oen, A. M. P., McClain, M. E., and Lopez-Gunn, E.: Nature-based solutions for hydro-meteorological risk reduction: a state-of-the-art review of the research area, *Natural Hazards and Earth System Sciences*, 20, 243–270, <https://doi.org/10.5194/nhess-20-243-2020>, 2020.
- 805 Sanford, G. R., Jackson, R. D., Booth, E. G., Hedtcke, J. L., and Picasso, V.: Perenniality and diversity drive output stability and resilience in a 26-year cropping systems experiment, *Field Crops Research*, 263, 108071, <https://doi.org/10.1016/j.fcr.2021.108071>, 2021.
- 810 Sohier, C.: Développement d'un modèle hydrologique sol et zone vadose afin d'évaluer l'impact des pollutions diffuses et des mesures d'atténuation sur la qualité des eaux en Région wallonne, *Development of a soil and vadose zone hydrological model to access impact of diffuses pollutions and mitigation measures on water quality in Walloon region*, 2011.



- Sowińska-Świerkosz, B. and García, J.: A new evaluation framework for nature-based solutions (NBS) projects based on the application of performance questions and indicators approach, *Science of The Total Environment*, 787, 147615, <https://doi.org/10.1016/j.scitotenv.2021.147615>, 2021.
- 815 Szabó, B., Weynants, M., and Weber, T. K. D.: Updated European hydraulic pedotransfer functions with communicated uncertainties in the predicted variables (euptfv2), *Geoscientific Model Development*, 14, 151–175, <https://doi.org/10.5194/gmd-14-151-2021>, 2021.
- Szabó, B., Kassai, P., Plunge, S., Nemes, A., Braun, P., Strauch, M., Witing, F., Mészáros, J., and Čerkasova, N.: Addressing soil data needs and data gaps in catchment-scale environmental modelling: the European perspective, *SOIL*, 10, 587–617, <https://doi.org/10.5194/soil-10-587-2024>, 2024.
- 820 Theeuwes, J. J. E., Staal, A., Tuinenburg, O. A., Hamelers, B. V. M., and Dekker, S. C.: Local moisture recycling across the globe, *Hydrology and Earth System Sciences*, 27, 1457–1476, <https://doi.org/10.5194/hess-27-1457-2023>, 2023.
- Toreti, A., Belward, A., Perez-Dominguez, I., Naumann, G., Luterbacher, J., Cronie, O., Seguni, L., Manfron, G., Lopez-Lozano, R., Baruth, B., van den Berg, M., Dentener, F., Ceglar, A., Chatzopoulos, T., and Zampieri, M.: The Exceptional 2018 European Water Seesaw Calls for Action on Adaptation, *Earth's Future*, 7, 652–663, <https://doi.org/10.1029/2019EF001170>, 2019.
- 825 Unger, P. W. and Kaspar, T. C.: Soil Compaction and Root Growth: A Review, *Agronomy Journal*, 86, 759–766, <https://doi.org/10.2134/agronj1994.00021962008600050004x>, 1994.
- Van Genuchten, M. Th.: A Closed-form Equation for Predicting the Hydraulic Conductivity of Unsaturated Soils, *Soil Science Society of America Journal*, 44, 892–898, <https://doi.org/10.2136/sssaj1980.03615995004400050002x>, 1980.
- 830 Vereecken, H., Amelung, W., Bauke, S. L., Bogaen, H., Brüggemann, N., Montzka, C., Vanderborght, J., Bechtold, M., Blöschl, G., Carminati, A., Javaux, M., Konings, A. G., Kusche, J., Neuweiler, I., Or, D., Steele-Dunne, S., Verhoef, A., Young, M., and Zhang, Y.: Soil hydrology in the Earth system, *Nat Rev Earth Environ*, 3, 573–587, <https://doi.org/10.1038/s43017-022-00324-6>, 2022.
- Wallace, E. E., McShane, G., Tych, W., Kretschmar, A., McCann, T., and Chappell, N. A.: The effect of hedgerow wild-margins on topsoil hydraulic properties, and overland-flow incidence, magnitude and water-quality, *Hydrological Processes*, 35, e14098, <https://doi.org/10.1002/hyp.14098>, 2021.
- 835 WALOUS 2018 - Série: <https://metawal.wallonie.be/geonetwork/srv/fre/catalog.search#/metadata/1c11ae54-f755-4d6c-95be-2e90c5c4fa70>, last access: 8 August 2024.
- Wastiaux, C.: Les tourbières sont-elles des éponges régularisant l'écoulement ?, *BSGLg*, 2008.
- 840 Weber, T. K. D., Weihermüller, L., Nemes, A., Bechtold, M., Degré, A., Diamantopoulos, E., Fatichi, S., Filipović, V., Gupta, S., Hohenbrink, T. L., Hirmas, D. R., Jackisch, C., de Jong van Lier, Q., Koestel, J., Lehmann, P., Marthews, T. R., Minasny, B., Pagel, H., van der Ploeg, M., Shojaezadeh, S. A., Svane, S. F., Szabó, B., Vereecken, H., Verhoef, A., Young, M., Zeng, Y., Zhang, Y., and Bonetti, S.: Hydro-pedotransfer functions: a roadmap for future development, *Hydrology and Earth System Sciences*, 28, 3391–3433, <https://doi.org/10.5194/hess-28-3391-2024>, 2024.
- 845 Wiecheteck, L. H., Giarola, N. F. B., de Lima, R. P., Tormena, C. A., Torres, L. C., and de Paula, A. L.: Comparing the classical permanent wilting point concept of soil (–15,000 hPa) to biological wilting of wheat and barley plants under contrasting soil textures, *Agricultural Water Management*, 230, 105965, <https://doi.org/10.1016/j.agwat.2019.105965>, 2020.



- van der Wiel, K., Batelaan, T. J., and Wanders, N.: Large increases of multi-year droughts in north-western Europe in a warmer climate, *Clim Dyn*, 60, 1781–1800, <https://doi.org/10.1007/s00382-022-06373-3>, 2023.
- 850 von Wilpert, K. and Schäffer, J.: Ecological effects of soil compaction and initial recovery dynamics: a preliminary study, *Eur J Forest Res*, 125, 129–138, <https://doi.org/10.1007/s10342-005-0108-0>, 2006.
- Wittwer, R. A., Klaus, V. H., Miranda Oliveira, E., Sun, Q., Liu, Y., Gilgen, A. K., Buchmann, N., and van der Heijden, M. G. A.: Limited capability of organic farming and conservation tillage to enhance agroecosystem resilience to severe drought, *Agricultural Systems*, 211, 103721, <https://doi.org/10.1016/j.agsy.2023.103721>, 2023.
- 855 Woolhiser, D. A., Smith, R. E., and Giraldez, J.-V.: Effects of Spatial Variability of Saturated Hydraulic Conductivity on Hortonian Overland Flow, *Water Resources Research*, 32, 671–678, <https://doi.org/10.1029/95WR03108>, 1996.
- XEVI, E., Christiaens, K., Espino, A., Sewnandan, W., Mallants, D., Sørensen, H., and Feyen, J.: Calibration, Validation and Sensitivity Analysis of the MIKE-SHE Model Using the Neuenkirchen Catchment as Case Study, *Water Resources Management*, 11, 219–242, <https://doi.org/10.1023/A:1007977521604>, 1997.
- 860 Yimer, E. A., De Trift, L., Lobkowicz, I., Villani, L., Nossent, J., and van Griensven, A.: The underexposed nature-based solutions: A critical state-of-art review on drought mitigation, *Journal of Environmental Management*, 352, 119903, <https://doi.org/10.1016/j.jenvman.2023.119903>, 2024.
- Zhang, M., Liu, N., Harper, R., Li, Q., Liu, K., Wei, X., Ning, D., Hou, Y., and Liu, S.: A global review on hydrological responses to forest change across multiple spatial scales: Importance of scale, climate, forest type and hydrological regime, *Journal of Hydrology*, 546, 44–59, <https://doi.org/10.1016/j.jhydrol.2016.12.040>, 2017.
- 865 Zhu, L., Fan, D., Ma, R., Zhang, Y., and Zha, Y.: Experimental and Numerical Investigations of Influence on Overland Flow and Water Infiltration by Fracture Networks in Soil, *Geofluids*, 2018, 7056858, <https://doi.org/10.1155/2018/7056858>, 2018.